Guidance and Control for Spinning, Gun-Launched Projectiles

L.J.N. van der Geest

Master of Science Thesis

TU Delft Delft University of Technology

Delft Center for Systems and Control

Guidance and Control for Spinning, Gun-Launched Projectiles

Master of Science Thesis

For the degree of Master of Science in Systems and Control at Delft University of Technology

L.J.N. van der Geest

February 18, 2019

Faculty of Mechanical, Maritime and Materials Engineering (3mE) · Delft University of Technology

The work in this thesis was supported by the Weapon Systems department of TNO. Their cooperation is hereby gratefully acknowledged.

Abstract

This thesis report is focused on the design of a guidance and control system that is able to minimize the deviation from the desired impact point for a firing range of 1 kilometer, given a 30mm spinning gun-launched projectile with a novel actuator design. This actuator is fixed on the projectile and offers a single force that can only be switched on or off.

In order to test the effectiveness of the guidance, navigation and control (GNC) system, an accurate model for both the projectile and the proposed actuator are constructed. These models will serve as a substitute for testing with working prototypes. The model for the projectile dynamics is constructed based on existing nonlinear six degrees of freedom (6-DOF) rigid-body models that are widely-used and validated. A new, simplified second order model that approximates the dynamics of the actuator, based on available measurements, is constructed.

The overall structure of the GNC loop is defined, with the guidance method of choice being the pre-calculation of a reference trajectory towards the intended target. This method serves to alleviate under-actuation and computation time problems. One of the most important contributions of the thesis is made with the description of a method for transforming the input from a single binary input signal towards two continuous virtual input forces. This method uses a discretization of the rolling motion of the projectile, such that an optimization can be done which results in a transformation from the binary on/off signal to two virtual force inputs. These two virtual force represent the steering forces in the directions perpendicular to the forwards motion that would have the same effect as the binary on/off signal if directly applied on the projectile.

The restructuring of the input allows for the use of PD-controllers to track the pre-defined trajectory. Using a grid-search method, the controller gains are found that best satisfy the design goal of minimizing the dispersion, which is defined by the sum of the mean error and the standard deviation of the impact points.

Analysis of the integrated solution shows that the proposed solution with the input transformation and the PD-controller is able to significantly reduce the projectile dispersion from standard deviations of about 50 cm to just a few cm. The exact performance depends on the frequency of the actuator and the spin rate of the projectile. The best performance is reached with high spin rates and actuator frequencies high enough to match these spin rates.

Table of Contents

List of Figures

List of Tables

Acknowledgements

I would like to thank my supervisor prof.dr.ir. J.W. van Wingerden for his assistance during the writing of this thesis. Even though I was often struggling, I always left our meetings motivated and eager to work on implementing some of the new ideas that you helped to form with your inspiration.

I would also like to thank my supervisor at TNO, ir. F. Bouquet, for allowing me to work on this inspiring project. Additional thanks are owed to him and the rest of the Weapon Systems department of TNO for providing a stimulating and comfortable working environment.

Delft, University of Technology
February 18, 2019

L.J.N. van der Geest

Chapter 1

Introduction

This chapter will give insights into the background of this thesis work. First a general introduction to the subject material is given, followed by a more in-depth explanation of the research goal and a further outline of the methodology and structure of the report.

1-1 General introduction

Since the conception of ranged munitions, effort has been put towards increasing their range and accuracy. In more specific terms: the goal has always been to improve the effective range; the range at which you are still able to accurately hit a target while also having an impact force strong enough to neutralize it. Over centuries, the need for increased effective range has led to the creation of many innovations in projectiles. New weapon systems as well as new types of ammunition followed.

1-1-1 Stabilization

In order to increase accuracy, especially at longer ranges, projectiles and missiles need to be stable. Stable in the sense that they will not flip over during flight. Flipping over increases the drag force and causes the projectile to be diverted in an unpredictable way, thus negatively impacting the performance. A common way to stabilize missiles and large projectiles is by adding fins to the body. This technique of fin-stabilization moves the center of pressure for the aerodynamic forces to the aft of the projectile body's center of mass (COM). This means that the increase of the angle of attack in a certain direction induces a moment in the opposite direction, thus making the missile inherently aerodynamically stable as shown in Figure 1-1.

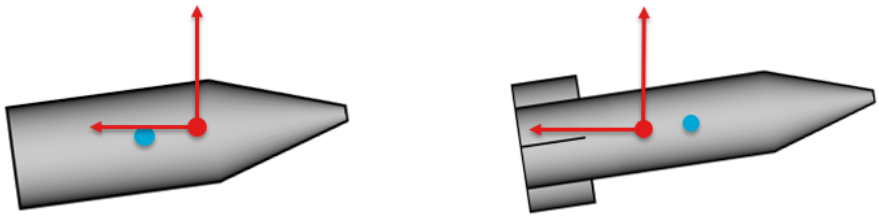

Figure 1-1: On the left an aerodynamically unstable projectile and on the right an aerodynamically stable projectile. In red the aerodynamic forces working at the center of pressure and in blue the projectile center of mass

Smaller gun-launched ammunition are more commonly spin-stabilized instead of fin-stabilized. This means that in order to provide stability to the inherently unstable projectiles, the projectile is spun around it's axis to provide a gyroscopic stabilizing effect during flight. The bullet is spun using helical grooves in the inner surface of a gun barrel, called rifling. Figure 1-2 gives an example of these grooves. The resulting spinning effect provides the stability and therefore accuracy for most gun launched projectiles.

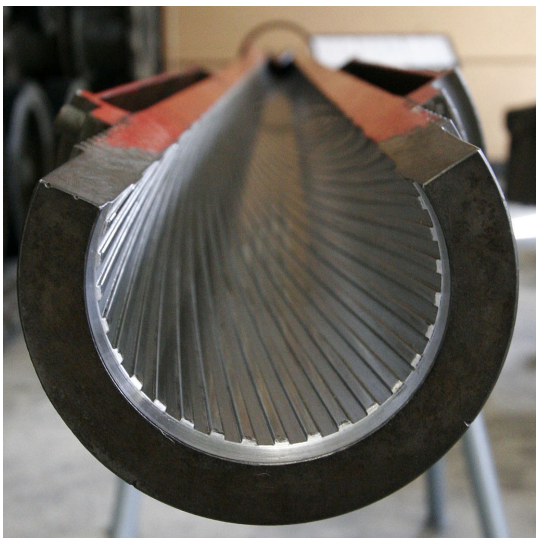

Figure 1-2: Rifling of a 105 mm Royal Ordnance L7 tank gun (2005). Retrieved from https://en.wikipedia.org/wiki/Rifling

1-1-2 Guided weapons

With stable projectiles, the effective range increases. However, with increasing firing range external effects such as wind, barrel-whip and powder charge variations will begin to cause non-negligible deviations from the desired projectile flight path. In addition, deviations caused by small aiming errors become more pronounced at larger distances. This loss of accuracy for longer ranges has led to the development of guided munitions starting in the last century. This field is commonly referred to as guidance, navigation and control (GNC). Developing smart,

guided projectiles would provide the ability to actively correct the flight trajectory; leading to better performance, lower ammunition spending and potentially less collateral damage.

Initially, the main focus was on the development of guided missiles. Extensive amounts of research and money has been invested towards developing new classes of guided weaponry, radio-controlled and laser-guided missile applications among those. The advancements in the field of smart missile systems were numerous and fast, while at the same time, similar developments for guided projectiles were lacking. Most missiles were fin-stabilized, which made it easy to directly control the direction of motion by manipulating the fins. High costs and unreliability have mostly prevented the use of similar guidance systems for smaller gun launched projectiles on the battlefield.

With the increasingly more available, cheaper and smaller sensors such as magnetometers and GPS, as well as the advances in computers being smaller and faster, in the last decades research on the control of projectiles has started to pick up. Many different control mechanisms have been developed, mostly involving the use small fins, which can be manipulated to change the attitude of the projectile. Using fins has a few downsides. The biggest one is that the resulting projectiles will be sub-caliber, meaning that the actual diameter of the projectile is smaller than diameter of the barrel on the launch mechanism. This means that launch mechanisms will be larger, heavier and more expensive. Furthermore, fins are very visible on enemy radar, increasing the risk for the soldiers using these weapon systems. Therefore research is needed to develop control strategies that are preferably without the use of fins.

1-1-3 Novel Actuator design

One of the companies currently working on guided projectiles is TNO. The Weapon Systems department at TNO has started the Innovative Projectile Control (IPC) project, which aims to offer a smart, low-cost solution for GNC of medium caliber projectiles. Medium caliber rounds are for example 30mm diameter rounds. The 30mm caliber is a specific size of autocannon ammunition, commonly used as anti-materiel or armor-piercing round. It is particularly effective against armored vehicles, as well as fortified positions. The 30mm caliber size includes the NATO standard 30x113mm rounds, most notably used in the M230 chain gun found on different types of attack helicopters such as the Apache. Another NATO standard size, 30x173mm rounds, are for example used in the Dutch Close-In Weapon System, Goalkeeper.

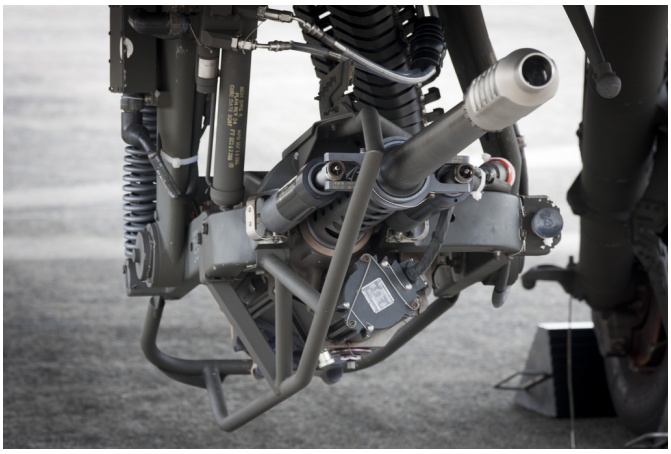

Figure 1-3: 30mm automatic Boeing M230 chain gun (2011). Retrieved from http://flickriver.com/photos/ah_kit/5772054279/

The research at TNO has so far been focused on developing a novel actuation system in order to apply control to medium caliber non-spinning projectiles. Specifically, a prototype for an actuation system without fins was developed. This prototype is capable of delivering a force perpendicular to the forward projectile motion as shown in Figure 1-4. The specifics of the actuator are discussed further in Chapter 2.

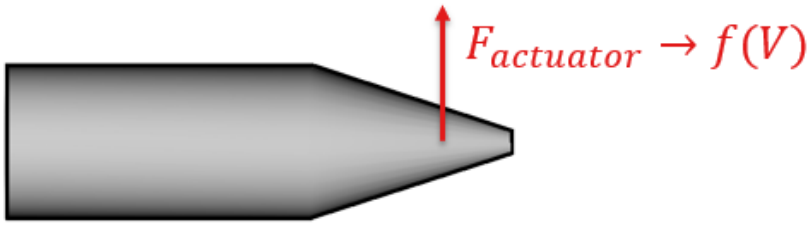

Figure 1-4: Schematic representation of the actuator force perpendicular to the forward motion

The current prototype is capable of stabilizing and controlling the angle of attack (AOA) for a non-spinning projectile. However, spinning projectiles are the norm in the current industry for these types of diameters. The use of non-spinning projectiles or fin-actuated projectiles would bring a need for investment and development in the launch mechanisms for these ammunition, making the cost of implementation very high. The desire is therefore to investigate the possibilities of this novel non-fin actuation solution for implementation in spinning projectiles of similar caliber size. If the actuator can be used to offer reasonable control to spinning projectiles, the system can be integrated with existing weapon systems and will effectively turn the conventional munitions into modern 'smart' munitions.

The remaining open issue is the design of GNC strategy for implementing this actuator in spinning projectiles. This thesis will therefore focus on developing a guidance and control strategy for the proposed actuated projectile in order to analyze the effectiveness, capabilities and feasibility of the actuator.

1-2 Problem statement

The problem statement that will be central to this thesis report is given as follows:

Given a medium-sized caliber spinning gun-launched projectile with an actuator developed by TNO, design a guidance and control system that is able to minimize the deviation from the desired impact point for a firing range of 1 kilometer.

In order to further clarify this statement some of the keywords mentioned can be explored as to their meaning and their justification:

- **Medium-sized:** With medium-sized, diameters in the range from $20 - 60$ mm are taken. These particular size projectiles are still large enough to fit actuating and sensor mechanisms inside and used in quantities small enough to justify the increased cost for a single projectile. For this thesis, specifically the diameter of 30mm is used, as the current prototype has been developed for a projectile of this size.
- **Gun-launched projectile:** Only projectiles without forward thrust during flight are taken into account. The projectile's only forward acceleration is during it's launch from the gun nozzle. Systems with forward acceleration during flight, such as missiles, are excluded for the sake of this research.
- **Impact point:** The impact point is the point at which the projectile collides with the ground or target. Specifically for this research, the impact point will be defined as the point where the projectile has travelled 1 kilometer downrange.
- **Firing range:** The firing range of 1 kilometer is chosen because medium caliber projectiles are often used up to ranges close to this. Short trajectories are excluded from investigation because the need for control is lower and the ability to offer meaningful control deviations is low because of the limited time. Longer range trajectories are also excluded for the sake of this research to avoid dealing with the transition from supersonic to subsonic flight.

1-2-1 Complexities

There are a few areas that offer the biggest challenges that make this particular type of projectile and actuator combination difficult to control. The main complicating factor is the high spin rates. The projectile spin rates are in the order of 10^3 rotations per second. This results in a few problems:

- The spinning motion, which helps to stabilize the projectile, resists the directional control. The actuator will be used to introduce an angle of attack, but the spinning motion will try to dampen this.
- In addition to resisting the control force in a single direction, the high spin rates makes it so that the dynamics for the pitching and yawing motion are coupled. This means that direction of the actuator force is not the same as the direction of the resulting motion response. Thus the equations of motion become highly nonlinear.

- Another problem that arises from the high spin rate is the need for fast reaction times in the control. As the actuator is fixed on the projectile, the ability to offer directional control is dependent on the reaction time of the actuator. With higher spin-rates, faster reaction times are needed.

Other complexities can be found that arise from the actuator design. The actuator is fixed on the projectile and offers a single force that can only be switched on or off. This offers more problems for the guidance and control design:

- The system is underactuated. The control objective is to minimize the deviation from the desired impact point. This is a point in three-dimensional space. Therefore we have a single actuator for the control of three degrees of freedom.
- The on/off control input results in an inability to directly use proportional control methods.
- The binary nature of the actuator also makes it so that the direction of control is dependent on the orientation of the projectile. Bringing a need for very accurate roll-orientation sensors and estimation strategies.

A final complicating factor is found in the lack of forward thrust. This means that as a result of steering the projectile the range will decrease. However, this is problem is small for the type of projectiles and firing ranges that are considered. Thus, no further attention will be placed on this topic.

1-3 Thesis overview and methodology

In order to provide a structured approach, for the purpose of this thesis the subject will be split into the following chapters:

Chapter 2: Projectile and Actuator Modeling

In order to eventually test the effectiveness of the guidance and control an accurate model for both the projectile and the proposed actuator must be constructed. These models will serve as a substitute for testing with working prototypes.

The projectile model will be based on existing models for projectile simulations, because these models are widely-used and validated. Therefore most attention will be placed on highlighting the areas specific to the projectile model for this thesis.

The actuator model cannot be based on established models. The proposed actuator is new and therefore requires the construction of a model. This thesis will focus on the design of a simplified model that can approximate the dynamics of the actuator based on measurements that are available from the prototype. A simplified model is chosen in order to avoid complex in-depth aerodynamic analyses, as the focus of this thesis is the control strategy.

Chapter 3: Guidance and Control structure

In this chapter, the structure of the GNC loop is defined. A description of the general structure is given followed by a quick note on the "Navigation" part in GNC. Thereafter, the guidance method is chosen based on a few of it's merits in comparison with other methods.

The most important part of the chapter focuses on the design of a method for transforming the control input from a single, binary input signal that defines the actuator state to two continuous virtual input forces. This method of transformation is explained in detail and serves to alleviate some of the problems that arise from the use of a single binary input for the control of multiple degrees of freedom.

Chapter 4: Controller

With the (re)structuring of the GNC loop in chapter 3 done, this chapter aims to offer a controller to be used in this loop. A case for the use of a PD-controller is made. The chapter will discuss how the controller is tuned and the results of the system will be analyzed.

Chapter 5: Integrated System Results

An analysis of the integration of the designed controller with the designed input transformation and the proposed actuator is done. The main focus is on the evaluation of the overall system performance. In addition, the influence of the actuator frequency as well as the spin rate is discussed.

Conclusion

The thesis report will end with a conclusion. This chapter will discuss the most important findings and contributions made in this thesis. Additionally a discussion of the applicability of the results and recommendations on further research are made.

Chapter 2

Projectile and Actuator Modeling

In order to eventually test the effectiveness of a guidance and control design, an accurate model of the projectile and the actuator must be created. These models will serve as a substitute for real-world testing. Therefore the models must be accurate enough to represent the dynamics of the system. This chapter will focus on the description of such a model for the projectile dynamics as well as the development of a model for the actuator dynamics.

2-1 Projectile Model

The system that has to be modeled is a 30mm diameter, symmetrical, spin-stabilized projectile flying under atmospheric conditions. Given a set of initial conditions, which include the initial velocity, spin rate, orientation and position, the projectile will follow a trajectory describing the evolution of these states. The acceleration and spin-up during launch is not modeled. Instead, the model starts with initial conditions representing the projectile states at the time where the projectile exits the gun muzzle.

The projectile model that is used in this thesis is based on existing and well-established nonlinear six degrees of freedom (6-DOF) rigid-body models for projectiles. These types of models offer a more accurate representation of the actual dynamics when compared to 3-DOF point-mass models or 4-DOF modified point-mass models, according to McCoy [1]. This is necessary because using a lower degree model would result in significant errors, especially in the calculation of the position. An accurate simulation of the position is very important as it ultimately describes the impact point, which is used in the calculation of the miss distance. The miss distance is the most important point in the simulation as it is used in the specification of the performance of the overall system.

2-1-1 Coordinate systems and projectile states

In order to describe the entire model, first, the states of the projectile have to be defined along with the reference frames that are to be used to describe these states in. The following states will be defined:

- **Position**: x, y and z describe the position of the projectile.
- **Orientation**: ϕ, θ and ψ describe the orientation of the projectile.
- **Velocity**: u, v and w describe the velocity of the projectile.
- **Angular velocity**: p, q and r describe the angular velocity of the projectile.

The position is described in an inertial coordinate system, defined as in Figure 2-1. The inertial right-handed coordinate reference frame is defined with it's origin located at the gun nozzle. The x coordinate describes the distance the projectile travelled downrange, the y coordinate describes the distance travelled perpendicular to the downrange distance and the z coordinate describes the height of the projectile, with z positive in the downwards direction. The positive direction of z defined as downwards is commonplace in existing literature on projectile control and attitude estimation. Therefore, this thesis will stick to that convention.

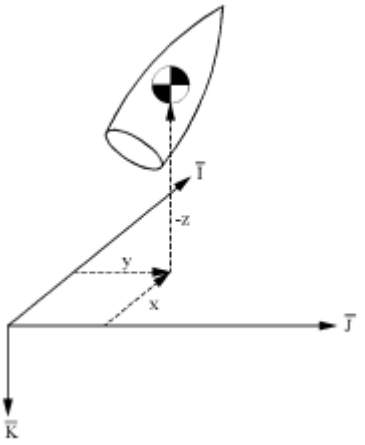

Figure 2-1: Projectile coordinate definition [2]

In addition to the inertial reference frame, a body-fixed reference frame is defined with the origin located at the center of mass (COM) of the projectile. This frame is important for the calculation of the aerodynamic moments and forces. These forces and moments in the body-fixed frame are used to calculate (angular) accelerations and velocities, which are then transformed using rotation matrices to the inertial frame in order to update the position. The rotation from the inertial frame to the body-fixed frame is described by the yaw-pitch-roll (YPR) Euler angle sequence (ψ, θ, ϕ) as in Figure 2-2.

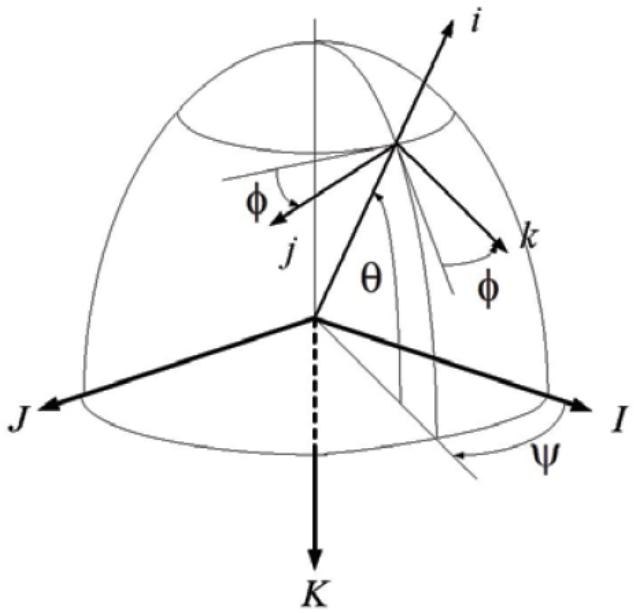

Figure 2-2: Earth-fixed and body-fixed systems and the Euler angle rotation [3]

In the case of this thesis, a non-rolling body-fixed frame is used. This means that the body-fixed frame doesn't rotate along with the rolling motion about the x-axis. Therefore, for the sake of the rotation matrices, roll angle $\phi = 0$. However, the value of ϕ is still updated as a state.

In this non-rolling body-fixed reference frame, the velocity components in body-x, y and z directions are given as u, v and w. The angular velocities of the projectile about these body-x, y and z axes are given by roll rate p, pitching rate q and yawing rate r respectively.

The trajectories that will be modelled are very flat. This means that the projectile is launched at very small inclines (low initial pitching angle θ). Furthermore the angle of attack (AOA) will stay close to zero during the flight, which also means that the yawing and pitching angles ψ and θ will be close to zero.

2-1-2 Nonlinear 6-DOF Rigid-Body Model

Using the definitions for the coordinate system and the states, the equations of motion can be defined. These equations of motion are widespread and can be found in studies done by Gkritzapis et al. [4] and Hainz and Costello [2]. These equations of motion are found in Equation 2-1 to 2-4.

$$\begin{bmatrix}\dot{x}\\ \dot{y}\\ \dot{z}\end{bmatrix} = \begin{bmatrix}\cos\theta\cos\psi & -\sin\psi & \sin\theta\cos\psi\\ \cos\theta\sin\psi & \cos\psi & \sin\theta\sin\psi\\ -\sin\theta & 0 & \cos\theta\end{bmatrix}\begin{bmatrix}u\\ v\\ w\end{bmatrix} \tag{2-1}$$

$$\begin{bmatrix}\dot{\phi}\\ \dot{\theta}\\ \dot{\psi}\end{bmatrix} = \begin{bmatrix}1 & 0 & \tan\theta\\ 0 & 1 & 0\\ 0 & 0 & 1/\cos\theta\end{bmatrix}\begin{bmatrix}p\\ q\\ r\end{bmatrix} \tag{2-2}$$

$$\begin{bmatrix}\dot{u}\\ \dot{v}\\ \dot{w}\end{bmatrix} = \frac{1}{m}\begin{bmatrix}F_x\\ F_y\\ F_z\end{bmatrix} - \begin{bmatrix}0 & -r & q\\ r & 0 & r\tan\theta\\ -q & -r\tan\theta & 0\end{bmatrix}\begin{bmatrix}u\\ v\\ w\end{bmatrix} \tag{2-3}$$

$$\begin{bmatrix}\dot{p}\\ \dot{q}\\ \dot{r}\end{bmatrix} = [I]^{-1}\left(\begin{bmatrix}M_x\\ M_y\\ M_z\end{bmatrix} - \begin{bmatrix}0 & -r & q\\ r & 0 & r\tan\theta\\ -q & -r\tan\theta & 0\end{bmatrix}[I]\begin{bmatrix}p\\ q\\ r\end{bmatrix}\right) \tag{2-4}$$

Equation 2-1 describes the evolution of the position using the velocities defined in the non-rolling body-fixed frame and a rotation matrix. Equation 2-2 does the same for the orientation using the angular rates from the same body frame. Equation 2-3 and 2-4 describe the evolution of the velocities and the angular rates in the body frame using the forces and moments that act on the projectile. These forces and moments are defined in Equation 2-5 and Equation 2-6.

$$\begin{bmatrix}F_x\\ F_y\\ F_z\end{bmatrix} = -\frac{1}{2}\rho V^2 A\begin{bmatrix}C_{X_0} + C_{X_2}\left(\frac{v^2+w^2}{V^2}\right)\\ C_{N_\alpha}(\frac{v}{V}) - \left(\frac{pd}{2V}\right)C_{Y_{p_\alpha}}(\frac{w}{V})\\ C_{N_\alpha}(\frac{w}{V}) + \left(\frac{pd}{2V}\right)C_{Y_{p_\alpha}}(\frac{v}{V})\end{bmatrix} + mg\begin{bmatrix}-\sin\theta\\ 0\\ \cos\theta\end{bmatrix} + F_a \tag{2-5}$$

$$\begin{bmatrix}M_x\\ M_y\\ M_z\end{bmatrix} = \frac{1}{2}\rho V^2 Ad\begin{bmatrix}\left(\frac{pd}{2V}\right)C_{l_p}\\ C_{M_\alpha}(\frac{w}{V}) + \left(\frac{qd}{2V}\right)C_{M_q} + \left(\frac{pd}{2V}\right)C_{N_{p_\alpha}}(\frac{v}{V})\\ -C_{M_\alpha}(\frac{v}{V}) + \left(\frac{rd}{2V}\right)C_{M_q} + \left(\frac{pd}{2V}\right)C_{N_{p_\alpha}}(\frac{w}{V})\end{bmatrix} + M_a \tag{2-6}$$

where:

$$\begin{aligned}\rho &= \text{density of air}\\ V = \sqrt{u^2+v^2+w^2} &= \text{total velocity}\\ A &= \text{cross-sectional area}\\ g &= \text{gravitational constant}\\ \frac{1}{2}\rho V^2 &= \text{dynamic pressure}\\ C_{X_0}, C_{X_2}, C_{N_\alpha}, C_{Y_{p_\alpha}}, C_{l_p}, C_{M_\alpha}, C_{M_q}, C_{N_{p_\alpha}} &= \text{aerodynamic coefficients}\\ F_a &= \text{actuator force}\\ M_a &= \text{actuator moment}\end{aligned}$$

The actuator force F_a and moment M_a will be discussed further in Section 2-2.

2-1-3 Aerodynamic Coefficients

The aerodynamic coefficients that are used to describe the aerodynamic forces and moments are specific to the projectile. They can usually be found empirically from windtunnel tests. Alternatively, they can be calculated by doing numerical analyses as are common in computational fluid dynamics (CFD) but they should be validated with experiments as numerical methods usually introduce slight inaccuracies. The aerodynamic coefficients used in this thesis are the following:

$$\begin{aligned} C_{X_0} &: \text{zero yaw axial force coefficient} \\ C_{X_2} &: \text{yaw axial force coefficient} \\ C_{N_\alpha} &: \text{normal force coefficient} \\ C_{Y_{p_\alpha}} &: \text{Magnus force coefficient} \\ C_{l_p} &: \text{spin damping moment coefficient.} \\ C_{M_\alpha} &: \text{overturning moment coefficient} \\ C_{N_{p_\alpha}} &: \text{Magnus moment coefficient} \end{aligned}$$

Important to note here is that the coefficients $C_{N_\alpha}, C_{Y_{p_\alpha}}, C_{M_\alpha}, C_{M_q}$ and $C_{N_{p_\alpha}}$ are equal in the y- and z-direction, because the projectile under consideration is symmetric.

In order to find the aerodynamic coefficients for the projectile in this thesis, the software package PRODAS (V2) by Arrow Tech was used. The projectile dimensions and materials were used to model the projectile in this software package. Using a combination of CFD data and empirical data from a large number of projectiles, PRODAS is able to predict the aerodynamic coefficients for Mach ranges from Mach 0 to Mach 8. The aerodynamic coefficients used in this report are therefore found by interpolating from tabulated PRODAS output data using the projectile velocity and the speed of sound to calculate the Mach number. Table B-1, with all the aerodynamic coefficients, is found in Appendix B.

2-1-4 Uncontrolled trajectory simulation

Using the model that has just been defined in Section 2-1-2, simulations can be done to show the model output. The initial conditions are used:

$x_0 = 0$ m	$\psi_0 = 0$ rad	$u_0 = 1000$ m/s	$p_0 = 6000$ rad/s
$y_0 = 0$ m	$\theta_0 = 0.0089$ rad	$v_0 = 0$ m/s	$q_0 = 0$ rad/s
$z_0 = 0$ m	$\phi_0 = 0$ rad	$w_0 = 0$ m/s	$r_0 = 0$ rad/s

The most important initial conditions are the varying ones: θ_0, ψ_0 and p_0. The initial condition of $u_0 = 1000$ m/s will be standard in this thesis as well as the other zero initial conditions. The spin rate $p_0 = 6000$ rad/s will be varied later on in order to investigate the influence on the actuator design criteria, the initial pitching and yawing angle will be varied as they represent the firing angle. For the simulations given in Figure 2-3, the pitching angle θ_0 is chosen such that the impact point at $x = 1000$ will be at height zero.

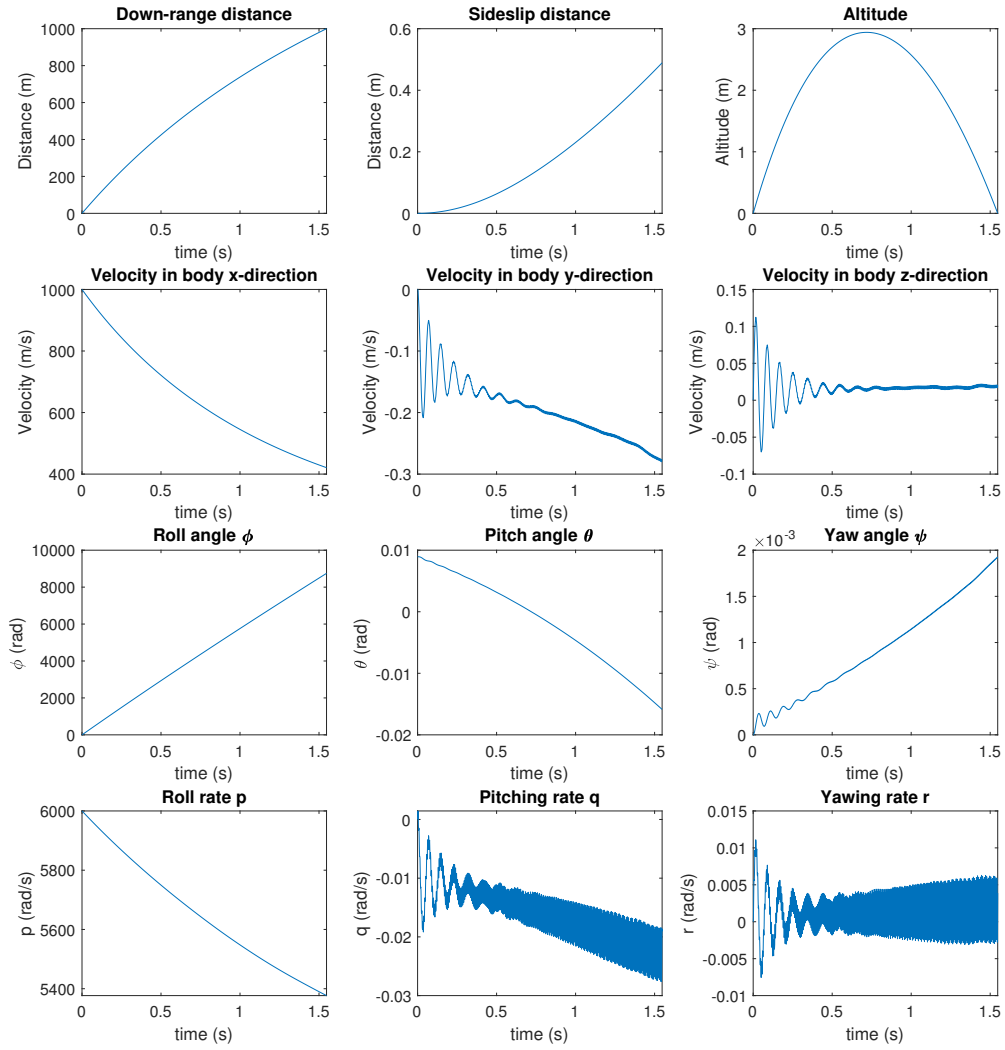

Figure 2-3: Simulation results for uncontrolled firing

From the simulation results in Figure 2-3, it can be seen that the projectile is diverted to the right during the flight. This is a result of the Magnus forces and the influence of the spinning effect. The position is also plotted in 3D in Figure 2-4 in order to show this effect.

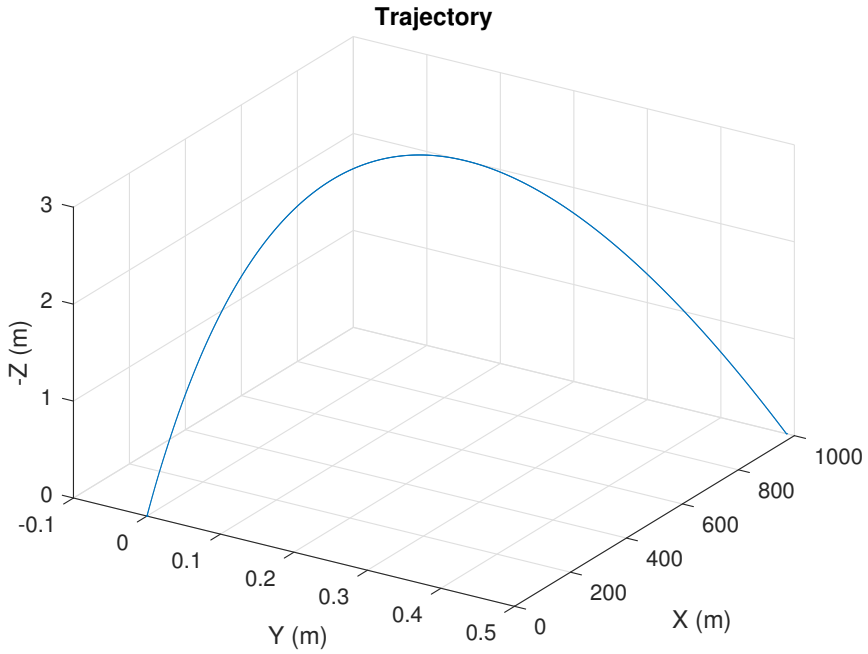

Figure 2-4: 3D plot of simulation result for an uncontrolled firing

These results are generated without any actuator input and just serve to highlight the general evolution of all of the projectile states.

2-2 Actuator modeling

As explained in Chapter 1, the actuator is capable of generating a force perpendicular to the forward motion. This is achieved by utilizing the stagnation point pressure. Using a ram-air intake at the tip of the projectile, the actuator is able to take in the incoming air at the stagnation point, which can then be diverted to an outlet on one of the sides. The difference between the high stagnation pressure at the tip and the pressure at the outlet of the divert channel results in a directional force. This force can then be toggled on or off by opening or closing the outlet. Figure 2-5 shows a schematic representation of this actuator system, integrated in the projectile.

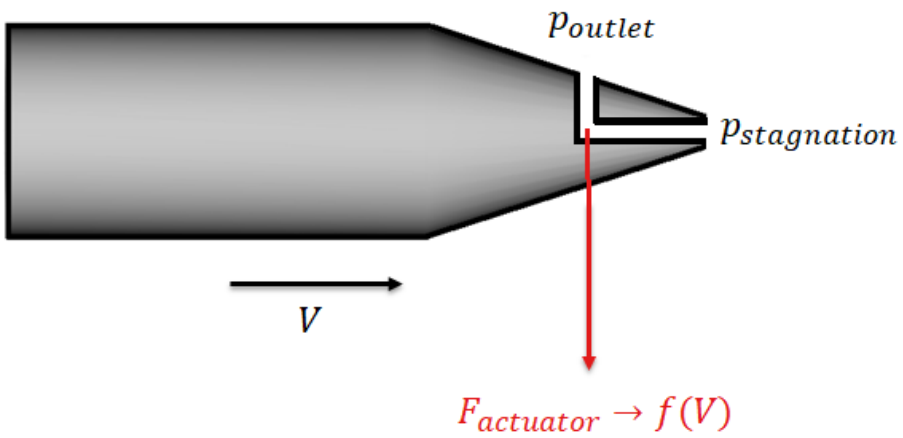

Figure 2-5: A schematic representation of the actuator

2-2-1 Actuator force magnitude

The stagnation point pressure can be approximated using the Bernouilli's equation [5] for inviscid, incompressible flows:

$$p + \frac{1}{2}\rho V^2 = const \tag{2-7}$$

Which, for the pressure at the stagnation point with $V_{stagnation} = 0$, amounts to

$$p_{stagnation} = \frac{1}{2}\rho V^2 + p_{static} \tag{2-8}$$

with:

$$\begin{aligned} \frac{1}{2}\rho V^2 &= \text{dynamic pressure} \\ \rho &= \text{density of air} \\ V &= \text{velocity of the projectile} \end{aligned}$$

This means that the generated force will be velocity-dependent, because it depends on the velocity-dependent stagnation point pressure. However the equations given above are not valid for the projectile as shock waves arise in this case. That means that the actual stagnation point pressure is lower, due to entropy production in the shock wave . The exact equations for this case can be found as for example on the NASA website [6].

The precise magnitude of the force can be calculated by doing an extensive analysis with the stagnation point pressure and the interaction between all of the different flows. For this thesis however, a simplified model of the actual force component, perpendicular to the velocity, will be used. Creating a highly accurate aerodynamic model is outside the scope of this research and for the proof of concept, a simplified model will suffice.

From an approximation of the stagnation point pressure with the Bernouilli equation, it can be estimated that the force will grow as roughly a quadratic function of the velocity. This

follows from the fact that the force is largely dependent on the difference between $p_{stagnation}$ and p_{outlet}, which will grow mostly depending due to the quadratic influence of the velocity in $p_{stagnation}$. Therefore measurements of the generated force for different velocities can be used in order to fit a simple second order model. The measurements, which are given in Table 2-1, have been collected using a prototype of the actuator and projectile system.

Mach	Force (N)
1.5	1.8
2.0	3.0
2.5	5.0
3.0	7.2

Table 2-1: Measured actuator force for different Mach numbers

The measurements are done by applying pressures at the intakes that simulate the stagnation point pressures that correlate to the given Mach numbers. The resulting force perpendicular to the forward motion is then measured and tabulated. Only a few data points were available for Mach numbers ranging from 1.5 to 3.0. As the typical velocity of the projectile is at most 1 km/s $\approx$ Mach 3, this should cover the range of relevant Mach numbers.

Now the quadratic polynomial in Equation 2-9 can be fitted to the measurements.

$$f_a(M) = a_1 M^2 + a_2 M + a_3 \tag{2-9}$$

where

$$M = \text{Mach number}$$

Using a least-squares fit the resulting coefficients a_1, a_2 and a_3 can be found:

$$\begin{aligned} a_1 &= 1.00 \\ a_2 &= -0.86 \\ a_3 &= 0.81 \end{aligned}$$

The final model for the actuator force as a function of the velocity is given in Equation 2-10.

$$f_a(V) = 1.00 \left(\frac{V}{c}\right)^2 - 0.86 \frac{V}{c} + 0.81 \tag{2-10}$$

with

$$c = \text{speed of sound}$$

Figure 2-6 shows a plot of the measurements and the model of the actuator force as a function of the Mach number.

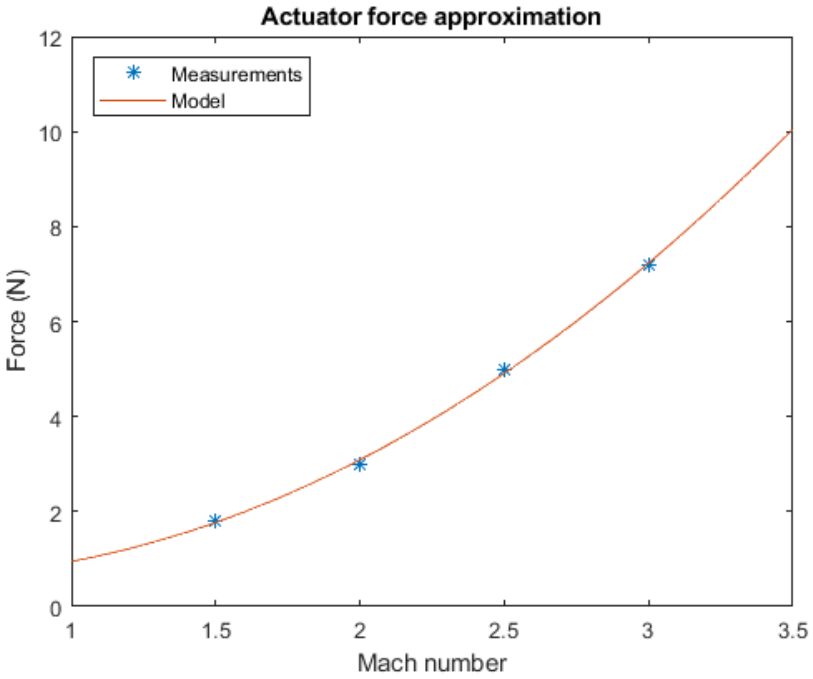

Figure 2-6: Actuator force magnitude model

2-2-2 Actuator force direction

Now that a model for the magnitude of the actuator force has been established, attention must be placed on the direction of the force. As the actuator is fixed to the projectile, the direction of the force is dependent on the Euler angles ϕ, θ and ψ. Since $\theta \approx 0$ and $\psi \approx 0$, the influence of these angles is negligible. Therefore the actuator force and the actuator moment can be described in the coordinate system defined in Chapter 2 as in Equation 2-11 and Equation 2-12 respectively.

$$F_a = \begin{bmatrix} F_{ax} \\ F_{ay} \\ F_{az} \end{bmatrix} = f_a(V) \begin{bmatrix} 0 \\ -\sin\phi \\ \cos\phi \end{bmatrix} u \tag{2-11}$$

$$M_a = \begin{bmatrix} M_{ax} \\ M_{ay} \\ M_{az} \end{bmatrix} = F_a(V) \times \begin{bmatrix} l \\ 0 \\ 0 \end{bmatrix} = f_a(V) l \begin{bmatrix} 0 \\ -\cos\phi \\ -\sin\phi \end{bmatrix} u \tag{2-12}$$

where

$$u \subset \{0, 1\} = \text{input}$$
$$l = \text{distance between the COM and actuator}$$

The actuator is now described by a single input u. This is a binary input describing the state of the actuator. The state is either 1 or 0, for on and off respectively. Describing the

input in this way is a simplification of reality. In reality, the actual manipulable variable is a voltage over an inductor. This inductor is part of a relais that is used to open or close the actuator outlet. The actuator state then switches between closed or open. The state u is then representing this state.

In actuality, this signal u can take values between 1 and 0, instead of being limited to just 1 and 0. However, the switch between an open and closed outlet is done in a time in the order of 10^{-5} s. Furthermore, the system cannot be put in a reliable intermediary state. Therefore the assumption is made that u only takes the values 0 and 1 for the remainder of the thesis.

The selection of the actuator state as the manipulable variable also means that the influence of any time delays that are present between the actual voltage input and the actuator state are excluded. The use of an inductor would introduce a delay between the Voltage input and the state of the actuator. Therefore, for the sake of the thesis this factor is excluded and the binary state u is taken as the direct control input.

Chapter 3

Guidance and Control structure

In this chapter, the structure of the guidance, navigation and control (GNC) loop will be analyzed. The specific problems for the GNC loop for this thesis will be highlighted. The guidance strategy that deals with some of these problems will be discussed.

Thereafter, a transformation of input will be made. The optimization problem that is solved to make this transformation is outlined. This transformation serves to eliminate some of the complexities that are present in the design process for the controller and is one of the main contributions of this thesis.

The chapter will conclude with an overview of the overall structure that leaves only the design of the controller to be discussed in Chapter 4.

3-1 GNC overview

As stated in Chapter 1, the goal of the thesis is the design of the guidance and control structure in order to minimize the deviation from the desired impact point. The general structure of the GNC systems that deal with these problems can be seen in Figure 3-1. Guidance refers to the determination of the preferred trajectory for the states to follow. The control issue deals with the manipulation of the control inputs in order to achieve the required performance based on the guidance commands. Navigation handles the measurement and estimation of the system states, such that guidance and control are made possible.

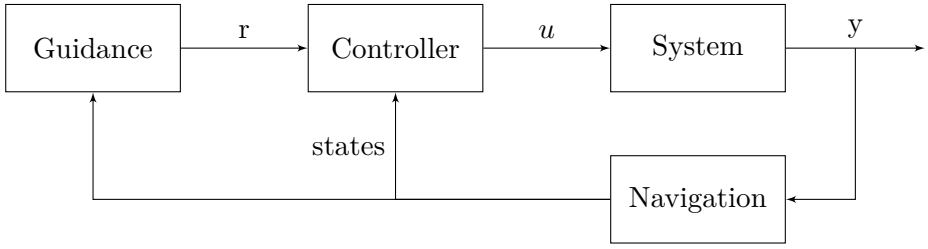

Figure 3-1: Guidance, Navigation and Control loop

3-1-1 A note on navigation

The specific focus of this thesis is place on guidance and control. The navigation part of the systems is also very important. Without proper design of sensors and estimation strategies, guidance and control are impossible. For fast spinning projectiles, this problem is especially pronounced.

Research on the topic of estimation is common. Research done on the use of different sensors for projectiles is available. Zhu et al. [7] and Rogers and Costello [8] describe the use of magnetometers as well as infrared sensors [9] for attitude estimation. Harkins and Hepner [10, 11] have also investigated the use of optical sensors for roll rate measurements.

The research for different estimation techniques is also readily available. Especially the Extended Kalman Filter (EKF) is studied in great detail for this task. Changey et al. [12], Rogers and Costello [3, 8, 9], Allik et al. [13] and Maley [14] offer research on the combination of different sensors with an EKF for state estimation, specifically for projectiles.

Because the research is already widely available and in order to limit the scope of the research, the assumption is made that perfect information on the projectile states is available. This assumption, which will be used for the remainder of the thesis, allows for a focus on the guidance and control part. This part of the equation is more interesting as the guidance and control strategy for this particular projectile and actuator combination differs from the design for other systems. The navigation strategies for different projectiles will all be very similar and can thus be based on the available research.

3-1-2 Guidance

The guidance of the projectile refers to the calculation of the preferred trajectory for the projectile to follow. In this case, the guidance commands should provide a trajectory that satisfies the objective of minimizing the deviation from the desired impact point. This impact point is defined at a point 1 km downrange of the firing of the projectile in the inertial reference frame from Section 2-1-1. The guidance commands should thus provide a trajectory that steers the projectile from it's launch point towards this desired impact point.

The launch point is fixed in the inertial reference frame at $(x_0, y_0, z_0) = (0, 0, 0)$. The desired impact point is defined as $(x_d, y_x, z_d) = (1000, 0, 0)$ in the inertial reference frame. The projectile is fired with initial velocity $u_0 = 1000$ m/s. Using this information and the projectile model defined in Chapter 2, the required initial pitch and yaw angle can be found, such that the nominal, undisturbed trajectory will end in the desired impact point. An example can be seen in Figure 3-2.

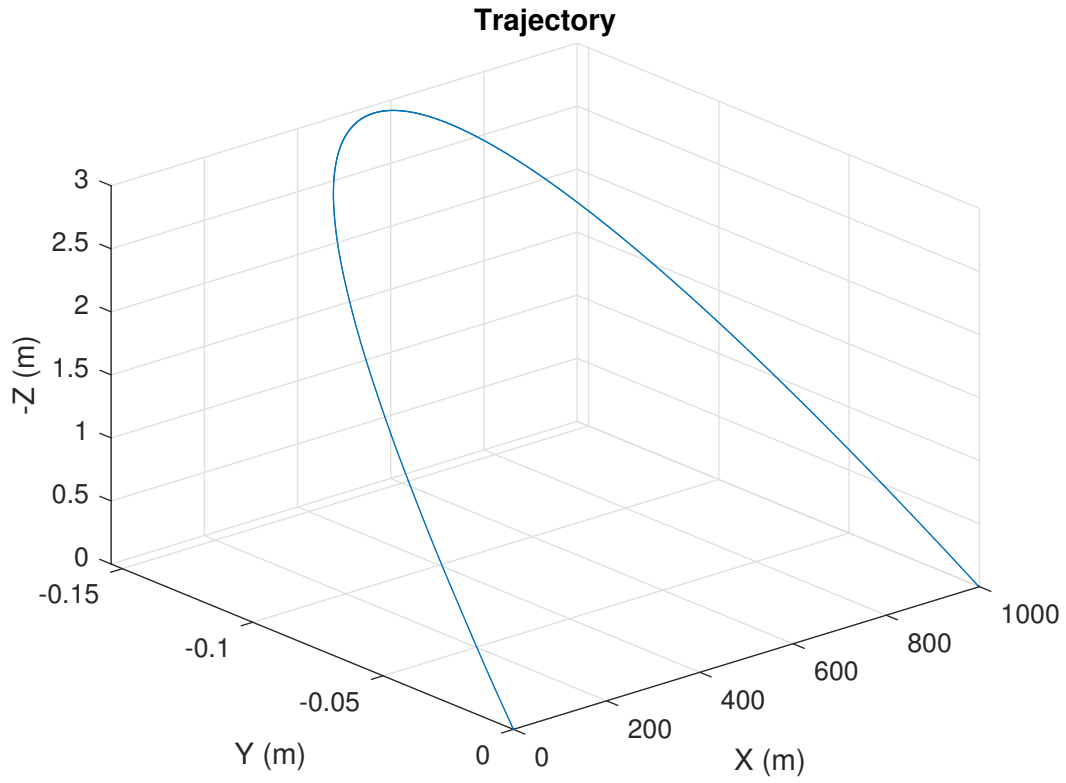

Figure 3-2: Pre-launc calculated undisturbed trajectory

This calculation of nominal undisturbed trajectories from launch point to impact point can be done before launching and saved as the reference trajectory. The goal of the controller is then to track this sequence of desired x, y and z coordinates. This guidance method with pre-launch trajectory calculation has a few distinct advantages when compared to other methods:

- A pre-launch calculation of the trajectory serves to eliminate a significant amount of computation time during flight. For this high velocity, high spin rate projectile, this is especially important. This makes this method preferred when compared to other guidance strategies using impact point prediction (IPP) based on a form of model predictive control (MPC) using the projectile model.
- The guidance commands automatically take into account the uncontrolled trajectory of the projectile. Other guidance strategies, such as proportional navigation guidance (PNG) [15], usually try to drive the line-of-sight angular rate between target and projectile to zero. This poses problems when the projectile has no forward thrust and sideslip as is the case for this projectile, which can be seen in Chapter 2.

Using the pre-launch calculated trajectory, the control problem transfers to the tracking of two degrees of freedom. This is achieved by using the current value of x to interpolate the desired values for y and z from the calculated trajectory. The implementation of this strategy can be seen in Figure 3-3.

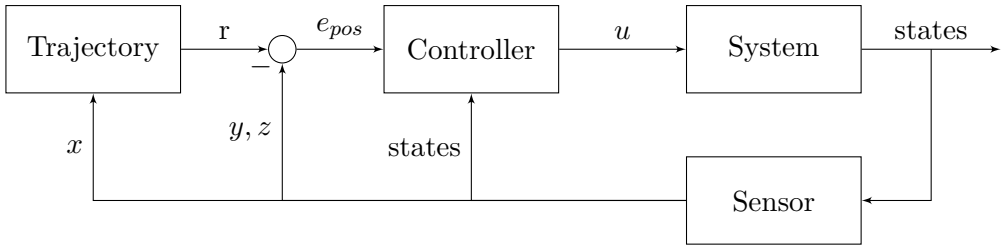

Figure 3-3: Overall guidance and control loop

This implementation can be thought of as serving to achieve one or both of two overall goals for the weapon system. On the one hand, the strategy can be used to calculate the desired initial firing angle defined by initial values for yaw ψ and pitch θ along with the nominal trajectory that follows from that. Essentially this is the planning of the desired aim and trajectory.

On the other hand, given a known initial firing angle, the system calculates the reference trajectory to follow such that the projectile actually arrives at the place where the system is aiming. This refers more to the reduction of the dispersion that results from various disturbances.

3-2 Actuator Transformation

With the guidance method specified in Section 3-1-2, the goal for the controller is following reference signals for the y and z coordinates by manipulating the input signal u. Using the formula for the actuator force in Equation 2-11, it can be seen that the signal u influences only the actuator forces in y and z direction. Therefore the actuator force can be restated as in Equation 3-1.

$$F_a = \begin{bmatrix} F_{ay} \\ F_{az} \end{bmatrix} = f_a(V) \begin{bmatrix} -\sin\phi \\ \cos\phi \end{bmatrix} u \tag{3-1}$$

The x direction is uncontrollable, but the choice of guidance strategy has also eliminated the need for controlling the x coordinate, so this is not a problem. However, there is still the issue of controlling the errors in the other directions with the single input u.

In order to solve this problem, a transformation will be made towards two virtual inputs that are more intuitively related to the y and z directions in which will be controlled, namely the actuator forces in these directions: F_{ay} and F_{az}. The forces are defined in the non-rolling body-fixed reference frame. The errors in the position are defined in the inertial frame. However, because the yaw and pitch angles are very small, the assumption is made that these directions are equal.

A transformation strategy will be outlined that makes the use of these virtual inputs as control inputs possible. The transformation, schematically shown in Figure 3-4, will calculate the actual input signal u, such that the effect on the projectile is equivalent to directly applying virtual inputs F_{ay} and F_{az}.

Figure 3-4: Transformation block

In order to transform the the F_{ay} and F_{az} signals into a single input u, this input must therefore describe both the magnitude and the direction of the actuator force. As u only takes values 0 and 1, the magnitude and direction cannot come from the variation of the value of u. Instead, the manipulation occurs by using a specific timing for the opening and closing actions of the actuator.

The direction of the force is influenced by an uncontrollable roll angle ϕ. By choosing to open or close the actuator only at certain values of ϕ, the direction can be influenced. By having the actuator open and close for varying amounts of time, the magnitude can also be varied. The solution for these timing problems can be restated as an optimization problem which will follow in the rest of the chapter.

3-2-1 Rolling motion discretization

The rolling motion of the projectile is described by the roll angle ϕ as defined in Chapter 2. Because the actuator is fixed to the projectile, the roll angle that describes the direction of the actuator force is the same angle ϕ. In order to make the transformation from the binary input signal u, this rolling motion is separated in roll cycles from 0 to 2π.

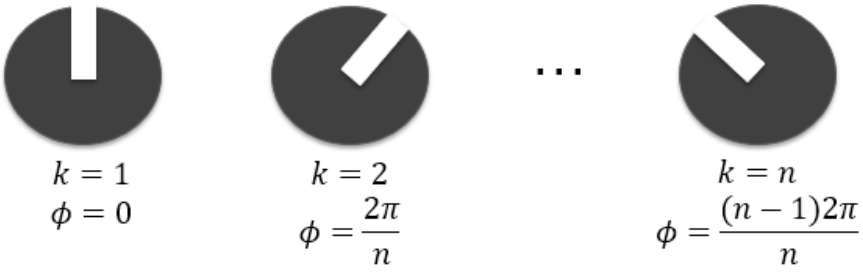

Figure 3-5: Actuator discretization of a single roll cycle, as seen from behind

The roll cycles from 0 to 2π can be split into discrete data points described by $k = 1$ to $k = n$, as shown in Figure 3-5. The signal u consists of n data points $u_1, u_2 \dots u_n$ that describes the signal during such a single roll cycle for each value of k.

3-2-2 Optimization problem

If a full signal u can be calculated such that the effective result of this input signal is equal to directly applying forces F_{ay} and F_{az} on the projectile, the transformation to these virtual inputs can be made. Using the definition of the actuator force as in Equation 3-1 and the

discretization from Section 3-2-1, the problem now becomes the optimization problem given in Equation 3-2.

$$\min_{u_1 \dots u_n} \left\| \begin{bmatrix} F_{ay} \\ F_{az} \end{bmatrix} - F_{res}(u) \right\|^2 \quad \text{s.t.} \quad u_1, u_2, \dots, u_n \subset \{0, 1\} \tag{3-2}$$

The force $F_{res}(u)$ is defined as in Equation 3-3.

$$F_{res}(u) = \frac{f_a(V)}{n} \begin{bmatrix} -\sin(0) \\ \cos(0) \end{bmatrix} u_1 + \frac{f_a(V)}{n} \begin{bmatrix} -\sin(\frac{2\pi}{n}) \\ \cos(\frac{2\pi}{n}) \end{bmatrix} u_2 + \dots + \frac{f_a(V)}{n} \begin{bmatrix} -\sin\left(\frac{(n-1)2\pi}{n}\right) \\ \cos\left(\frac{(n-1)2\pi}{n}\right) \end{bmatrix} u_n \tag{3-3}$$

This force $F_{res}(u)$ is the resultant force found from combining the n different actuator forces at each of the n different data points of a single roll. The resultant force F_{res} can only reach magnitudes up to $\frac{2}{2\pi} f_a(V)$, which follows from the following observations:

- If the force was in the right direction during the entire roll cycle, the resultant force can be as high as the actuator magnitude:

$$f_a(V)$$

- The actual maximum magnitude in a single direction is reached by activating the actuator during only the desired half of the roll. The maximum average magnitude in a single direction is then is given by:

$$\frac{f_a(V)}{2\pi} \left(\int_0^{\pi} sin\phi d\phi + \int_{\pi}^{2\pi} 0 d\phi \right) = \frac{2}{2\pi} f_a(V) \tag{3-4}$$

3-2-3 Input constraints

There are extra limitations that need to be placed on the input signal u. As discussed in Section 2-2, the possible values between 0 and 1 and the time delay resulting from the use of an inductor are not taken into account for this thesis. However, there is a significant limitation on the time between opening and closing. The maximum reaction time of the actuator determines the minimum time the actuator has to stay open when opened or close when closed. Therefore not all input signals $u_1, u_2, \dots, u_n$ will be feasible.

The minimal period of the actuator and the value of u within that period, schematically shown in Figure 3-6, are defined by two values: minimum period length T_{min} and minimum time opened t_{open}. This also implicitly specifies the minimum time closed t_{closed}.

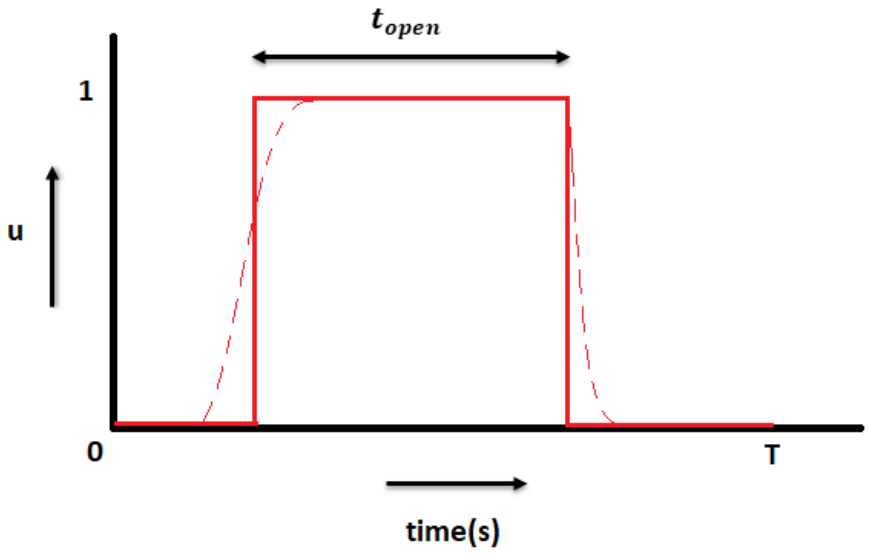

Figure 3-6: Minimal actuator period. The dotted red line represents a more realistic cycle and the solid line represents the model using the assumption of binary values.

As a rule of thumb, the minimum time open is chosen as $0.4T_{min}$ for the remainder of the thesis. This value follows from observations made on actuator tests with the existing prototype. Using this value, the complete structure of the actuator period is defined by the minimum period length T_{min} and thus by the maximum actuator frequency f_{max}:

$$T_{min} = \frac{1}{f_{max}}$$
$$t_{open} = \frac{0.4}{f_{max}}$$
$$t_{closed} = \frac{0.6}{f_{max}}$$

Therefore the optimization should only offer a result that is consistent with these timings. These timings can be converted into discrete steps of the roll cycle:

- The duration of a single timestep is defined by the total number of steps n and the current spin rate $p(t)$:

$$\Delta t = \frac{2\pi}{p(t)n}$$

- The minimum amount of consecutive steps the actuator needs to stay open is then defined:

$$\Delta k_{open} = \left\lceil \frac{t_{open}}{\Delta t} \right\rceil \tag{3-5}$$

For an example using $n = 5$, $p(t) = 2\pi$ and $f = 1$:

$$T_{min} = \frac{1}{f} = 1$$
$$\Delta t = \frac{2\pi}{p(t)n} = 0.2$$
$$\Delta k_{open} = \left\lceil \frac{0.4T_{min}}{\Delta t} \right\rceil = 2$$
$$\Delta k_{closed} = \left\lceil \frac{0.6T_{min}}{\Delta t} \right\rceil = 3$$

Then the only feasible signals u are:

$$\begin{bmatrix} u_1 \\ u_2 \\ u_3 \\ u_4 \\ u_5 \end{bmatrix} = \begin{bmatrix} 0 \\ 0 \\ 0 \\ 0 \\ 0 \end{bmatrix}, \begin{bmatrix} 1 \\ 1 \\ 0 \\ 0 \\ 0 \end{bmatrix}, \begin{bmatrix} 0 \\ 1 \\ 1 \\ 0 \\ 0 \end{bmatrix}, \begin{bmatrix} 0 \\ 0 \\ 1 \\ 1 \\ 0 \end{bmatrix}, \begin{bmatrix} 0 \\ 0 \\ 0 \\ 1 \\ 1 \end{bmatrix} \text{ or } \begin{bmatrix} 1 \\ 0 \\ 0 \\ 0 \\ 1 \end{bmatrix}$$

This immediately shows one of the shortcomings of an optimization over a single roll cycle. If the actuator frequency is too low to fit a minimum period in a single roll cycle, the only feasible signal will be a zero-signal. In reality, it is also possible to generate a directional force when spreading the signal over two or more roll cycles.

The minimum amount of roll cycles needed to fit the minimum period T_{min} is dependent on the maximum actuator frequency f and the current roll rate $p(t)$. This minimum amount is given by

$$N_{min} = \left\lceil \frac{p(t)}{2\pi f} \right\rceil \tag{3-6}$$

The current prototype is capable of actuating at a frequency of 400 Hz and the roll rates are about 6000 rad/s, the minimum required roll cycles for the optimization is

$$N_{min} = \left\lceil \frac{6000}{800\pi} \right\rceil = 3 \tag{3-7}$$

For combinations that are more favorable and that can be fitted within a single roll cycles, signals that are spread over multiple roll cycles are also possible. In order to have the optimization consider all these possibilities, the optimization will be done over a 6 roll window. As multiples of 1,2 and 3 can fit within this amount.

Although there is now a possibility of mapping an actuator signal that requires the time of 3 full roll cycles, the maximum magnitude of the force that can be reached with this signal is lower. Where the maximum force for mapping on a single roll cycles was given in Equation 3-2-2 as $\frac{2}{2\pi} f_a(V)$, the maximum directional actuator force when requiring a larger amount of roll cycles N for a single actuator period is given by:

$$\frac{2}{2\pi N} f_a(V) \tag{3-8}$$

3-3 Implementation

All possible periodic signals for mappings over 1, 2 or 3 roll cycles are generated and used to calculate the corresponding average actuator force $F_{res}(u)$. The resulting force that minimizes

$$\left\| \begin{bmatrix} F_{ay} \\ F_{az} \end{bmatrix} - F_{res}(u) \right\|^2$$

is found and the signal u that generates this forces is chosen as the actuator input. The current required actuator state is found by interpolating with the optimization result using the current roll angle ϕ. This process is repeated every 0.01s. This amount is chosen because with roll rates in the order of 5000-6000 rad/s, the time of a single roll is in the order of $1e^{-3}$ s. This way, at least a full 6 roll optimization sequence fits within the time before the next input update. Additionally, a choice for a smaller time between updates will increase the computational load.

An example of the approximation of forces in y and z directions is given in Figure 3-7.

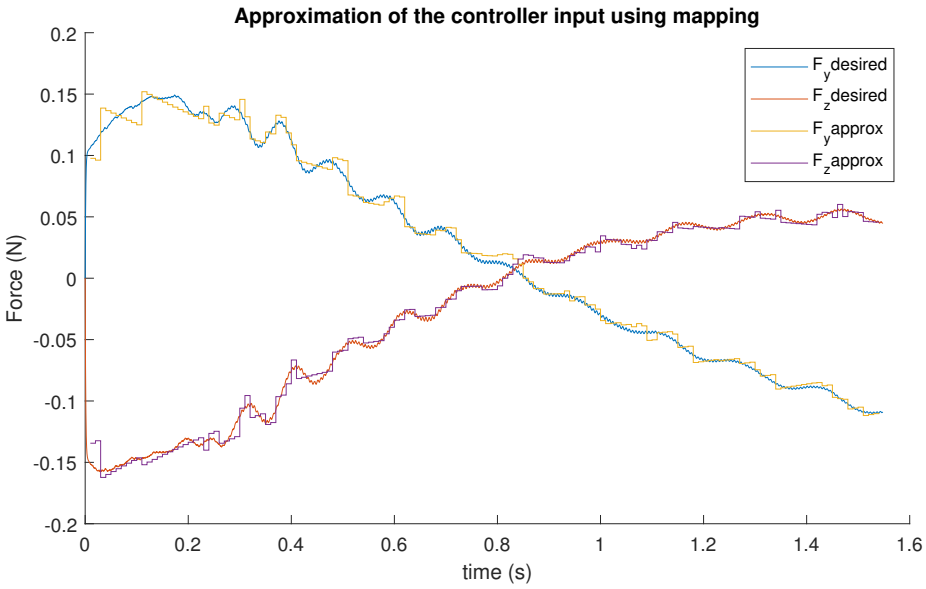

Figure 3-7: Input approximation

Figure 3-8 shows a small part of the same approximation as in Figure 3-7. The lower graph in the figure also shows the actual input signal that results in the approximation shown in the upper part of the figure.

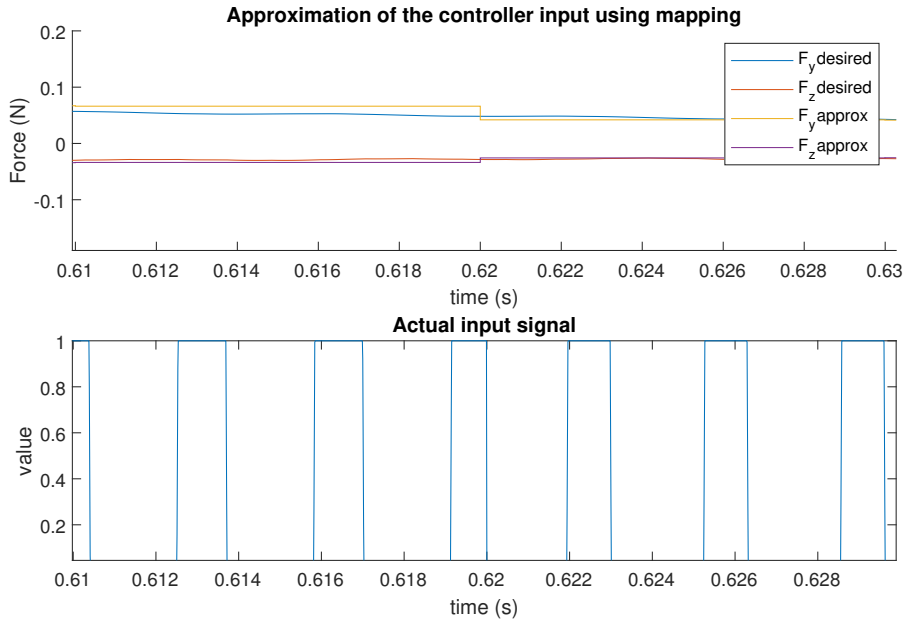

Figure 3-8: Input approximation with the corresponding actual input signal u.

With the transformation from the virtual inputs F_{ay} and F_{az} possible, the overall GNC loop can now be shown as in the block-scheme of Figure 3-9. The remaining issue is the design of the controller to calculate the required virtual inputs.

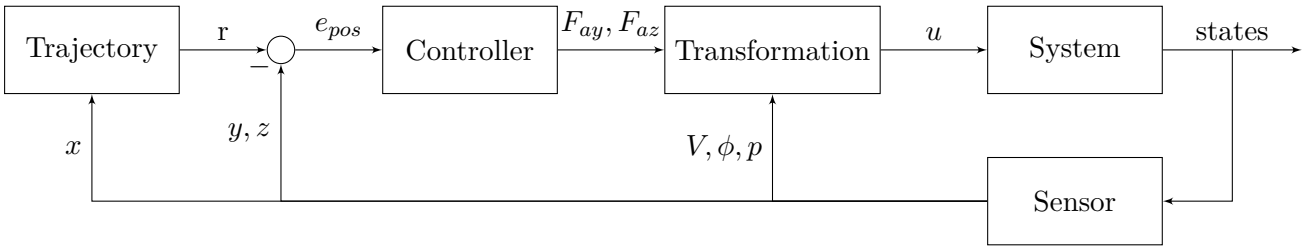

Figure 3-9: Control loop augmented with an input transformation

Chapter 4

Controller

With the (re)structuring of the guidance, navigation and control (GNC) loop in chapter 3 done, this chapter aims to offer a controller to be used in this loop. The chapter starts with a discussion of the control objective along with the definition of the performance of the controller. Thereafter the choice for a PD-controller is discussed followed by the tuning of the controller gains for this controller.

The chapter ends with an overview of the performance of the overall system and the influence of the actuator frequency and the spin rate on the performance.

4-1 Control objective

The guidance strategy was defined in Chapter 3, where the goal is to follow a reference trajectory as in Figure 3-2 for example. The tracking errors that need to be controlled by the controller can be seen in Figure 4-1. Here, the red dot represents the y and z coordinates in the predefined trajectory that correspond to the current x coordinate and the blue dot represents the actual position of the projectile. The errors in these directions are given by e_y and e_z.

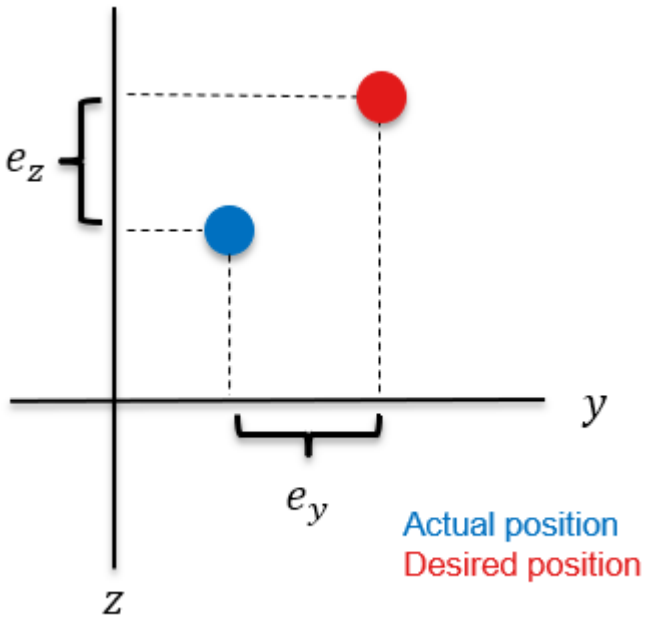

Figure 4-1: Tracking errors in y and z direction

The errors will be introduced in the system by introducing a variation in the initial conditions. These randomized irregularities represent the errors resulting from various system variables such as varying powder charge, weapon tolerances, sensor noise in initial aiming angles, etc. Errors resulting from atmospheric disturbances such as wind and temperature differences are not taken into account for this thesis. In order to introduce these errors into the simulations the following statements are applied:

- The projectile is fired with average initial yaw and pitch angles μ_ψ and μ_θ, such that the nominal, undisturbed trajectory will impact at the desired impact point as discussed in Chapter 3.
- These initial yaw and pitch angles will be disturbed, such that the actual initial angles are normally distributed variables:

$$\psi_0 \sim \mathcal{N}(\mu_\psi, \sigma^2) \tag{4-1}$$
$$\theta_0 \sim \mathcal{N}(\mu_\theta, \sigma^2) \tag{4-2}$$

- The value σ represents the dispersion of the weapon system in rad, resulting from the internal system variations as discussed. The value of σ is chosen based on common values for the dispersion of different 30mm projectiles. The value is chosen $\sigma = 0.8$ milliradians.

Using the errors introduced, the projectile impacts will be centered around the intended target impact point. The controller will work on reducing these tracking errors during flight, thus

returning the projectile to it's intended target trajectory and towards the intended impact point.

As stated in Chapter 1, the goal of the thesis is the design of a GNC system that is able to minimize the deviation from the desired impact point. This deviation consists of the accuracy and the dispersion. The accuracy is defined by the distance between the target and the average impact point, whereas the dispersion is defined by the variance around the average impact point. Therefore, with the rest of the system defined, the performance of the controller will be specified by a combination of the average error and the standard deviation:

$$J = \mu_{e_i} + \sigma_i \tag{4-3}$$

with:

$$\begin{aligned} \mu_{e_i} &= \text{average miss distance} \\ \sigma_i &= \text{standard deviation of impacts} \end{aligned}$$

The goal is to seek a controller that minimizes this cost function J. The measured averages and standard deviations that make up this performance indicator will all be based on simulations consisting of 50 firings using the normally distributed initial firing angles.

4-2 Controller choice

The controller must reduce the errors e_y and e_z during flight. With the help of the input transformation made in Chapter 3, the inputs available are forces in the same directions: F_{ay} and F_{az}. First, however, an observation must be discussed on the direction of these control forces.

4-2-1 Swerve response phase shift

During testing of the input in the model, the observation was made that the direction of the actuator force on the projectile is not equal to the direction of the resulting position response. This response, called the swerve response, is significantly shifted in phase. Figure 4-2 and Figure 4-3 highlight this fact.

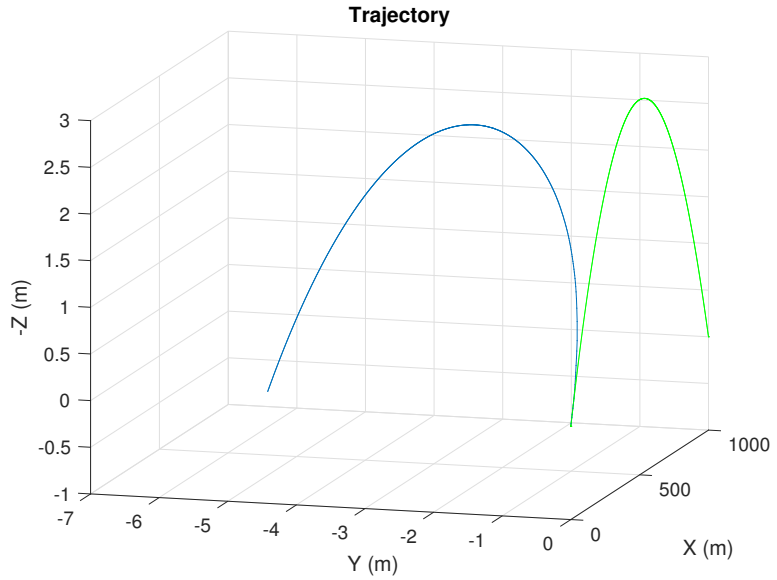

Figure 4-2: Swerve response to constant 1N control force in +y direction. The green line is the uncontrolled trajectory, the blue line the controlled trajectory

Figure 4-2 shows the swerve response of a projectile subjected to a control force of 1N in the positive y direction. The resulting trajectory ends in an impact point, which is diverted in a direction that differs from the positive y direction by 172.53°.

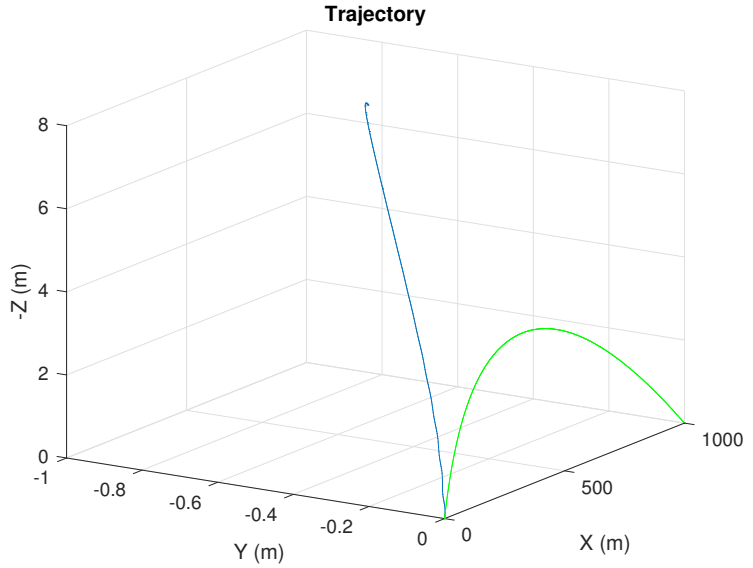

Figure 4-3: Swerve response to constant 1N control force in +z direction. The green line is the uncontrolled trajectory, the blue line the controlled trajectory

Figure 4-2 similarly shows the swerve response of a projectile subjected to a control force of 1N in the positive z direction. The resulting trajectory ends in an impact point, which is

diverted in a direction that differs from the positive z direction by 172.58°.

These observations are corroborated by and explained in further detail in the research done by Ollerenshaw and Costello [16] on the swerve response of projectiles to control input. They explain that for spin-stabilized projectiles, the swerve response to a control force applied in front of the aerodynamic center of pressure will undergo a phase shift approaching 180 degrees out of phase with the direction of the applied force.

Therefore, if the control forces are to be used for reducing the error in a particular direction, this phase shift must be taken into account.

4-2-2 PD Controller

With the errors e_y,e_z and the forces F_{ay},F_{az}, a logical choice of controller is the PD controller. In particular, a separate PD controller for both the y and z direction. The PD controller is defined by the transfer function:

$$K(s) = K_p + K_d s \tag{4-4}$$

Because of the symmetry of the projectile and the fact that the single actuator generates the forces, the controller gains for the two separate PD-controllers are chosen to be equal. The overall transfer function that takes the two errors e_y and e_z as input and outputs the virtual force inputs F_{ay} and F_{az} is then given in Equation 4-5

$$K(s) = \begin{bmatrix} K_p + K_d s & 0 \\ 0 & K_p + K_d s \end{bmatrix} \tag{4-5}$$

As seen in Section 4-2-1, the result of a control force in the positive y direction is almost completely in the negative y direction and equivalently for the force in positive z direction. When the small effect in the other direction is neglected, separate PD control loops for the different directions can be made as in Figure 4-4, with a similar loop for the z direction.

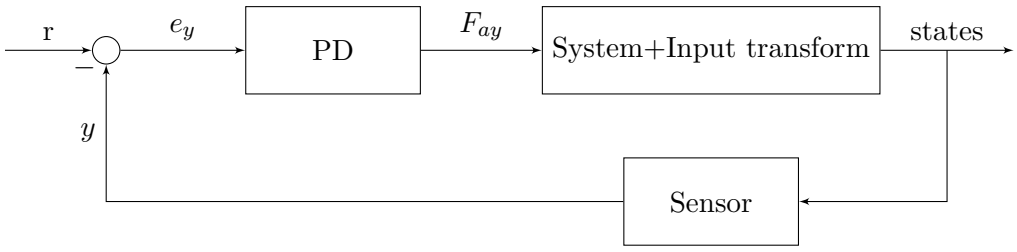

Figure 4-4: PD control loop for y direction

Here, the gains of the PD controller are chosen to be negative. This will ensure that the controller output will be in the opposite direction as the required swerve response as is required following the phase shift discussed earlier.

The most important benefit of this type of controller is the fact that it can easily be tuned using a grid-search for the controller gains K_p and K_d that make up the controller. Linear and model-based controllers are not preferred because the linearization of the model is not straightforward. In addition, it is difficult to compute the system matrices that are required for the calculation for optimal control techniques. The (non)linear system matrices are dependent on a few parameters and have to be updated on the fly for use in optimal control or model-based control.

Furthermore, the cost function J that represent the performance of the projectile is not directly related to the tracking behaviour of the controller. Because the cost function is based on an average of 50 simulations, the use of a grid-search method for the tuning of a PD controller makes sense. It allows for the selection of the specific controller gains that achieve this overall goal best based on simulation runs of 50 firings.

4-3 Controller tuning using grid-search

In order to find the controller gains that minimize the cost function J from Equation 4-3, a grid is defined containing values for the proportional controller gain K_p and derivative controller gain K_d. After an initial broader search, the grid is limited to the following values:

$$K_p = 0, -0.2, -0.4, \cdots, -4$$
$$K_d = 0, -0.1, -0.2, \cdots, -2$$

For every combination in the grid, 50 simulations are done. These simulations are done using the following principles:

- The projectile model from Chapter 2 is initialized with the following initial conditions:

$$\begin{aligned} x_0 &= 0 \\ y_0 &= 0 \\ z_0 &= 0 \\ \psi_0 &\sim \mathcal{N}(0.0089,\, 0.0008^2) \\ \theta_0 &\sim \mathcal{N}(-0.0005,\, 0.0008^2) \\ \phi_0 &= 0 \\ u_0 &= 1000 \\ v_0 &= 0 \\ w_0 &= 0 \\ p_0 &= 6000 \\ q_0 &= 0 \\ r_0 &= 0 \end{aligned}$$

- The trajectory to be tracked is the undisturbed trajectory that ends in the point $(1000, 0, 0)$.

- No external disturbances

- The forces that follow from the PD controller output are directly applied on the projectile, without the intermediate transformation and simulation of the actuator input. This allows for lower computation time and the elimination of any influence this transformation has on the control calculation

After the simulation of 50 firings according to these conditions, the average miss distance of the 50 firings μ_{e_i} and the standard deviation of the 50 impacts σ_i are computed. The sum of these is the value of the cost function J. The results for this search are given in Figure 4-5.

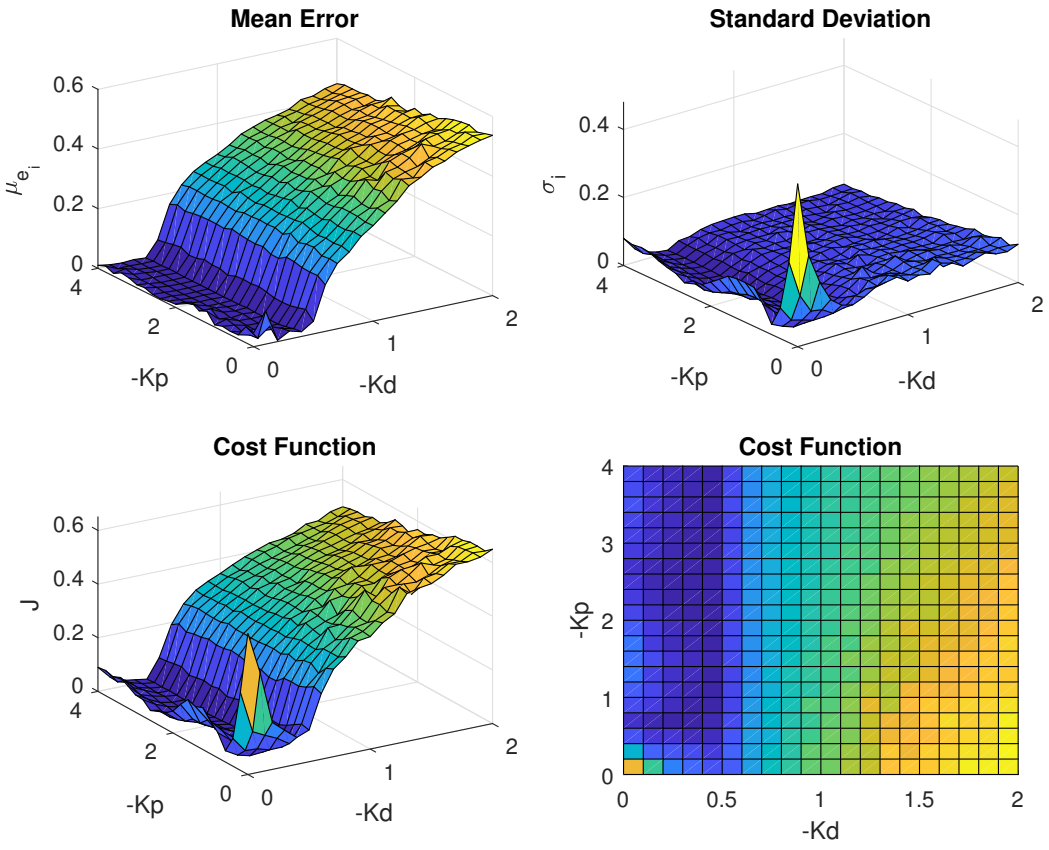

Figure 4-5: Grid search for optimal PD-gains

From the results the optimal $K_d = -0.4$ can be found. It is also visible in the figure that the variation of the proportional gain offer much less of an impact on the cost function than the variation of the derivative gain. This can be explained by looking at the influence of the controller gains on the shape of the trajectories.

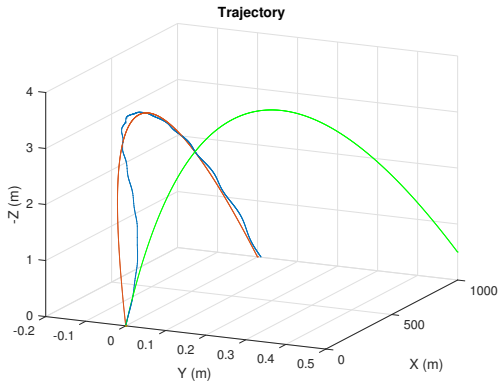

Figure 4-6: High K_p trajectory: $K_p = -4$, $K_d = -0.4$

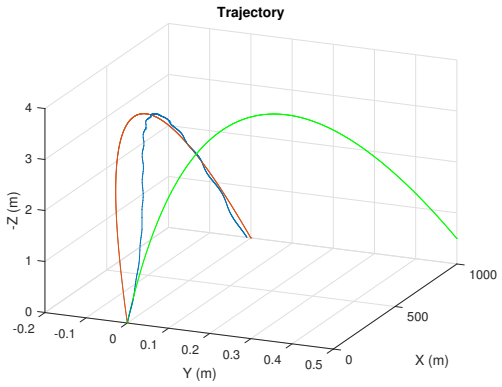

Figure 4-7: Low K_p trajectory: $K_p = -1$, $K_d = -0.4$

Figure 4-6 and Figure 4-7 show the trajectories for a higher or lower K_p respectively. The red trajectory represents the target, the green trajectory the uncontrolled trajectory and the blue trajectory is the controlled trajectory. Both figures are generated using the same initial conditions and the same optimal value for K_d. The value of K_p mainly influences the time it takes to converge to the desired trajectory. As the cost function does not value a faster convergence, the influence of the proportional gain on the performance is low.

Conversely, Figure 4-8 and Figure 4-9 show the trajectories for a higher or lower K_d respectively for the same initial conditions. Here it is clear that a K_d that is too high will cause the projectile to overcompensate for it's velocity and therefore start to oscillate. This increases the impact point error. On the other side a K_d that is too low will cause the projectile to under-compensate for it's velocity, therefore increasing the overshoot and settling time and increasing the impact point error.

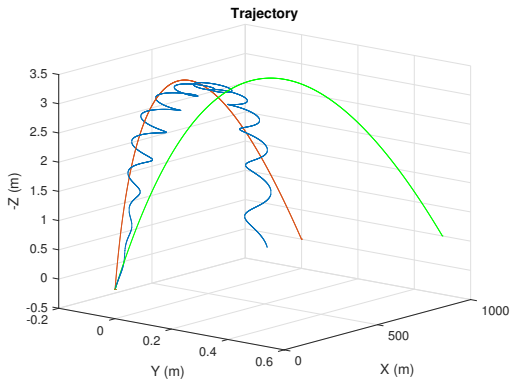

Figure 4-8: High K_d trajectory: $K_p = -4$, $K_d = -1$

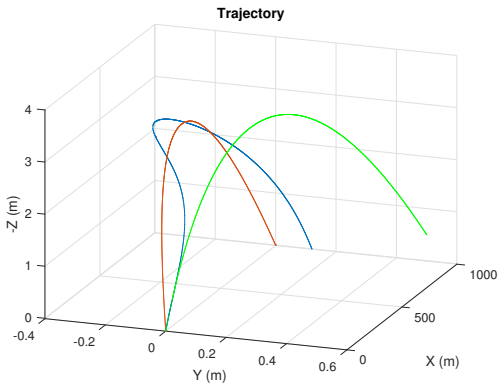

Figure 4-9: Low K_d trajectory: $K_p = -4$, $K_d = 0$

In general, a faster settling time is preferred for two main reasons:

- A faster settling time also implies the feasibility of the system for implementation on shorter distances than 1km.

- The maximum magnitude that can be generated is dependent on the velocity as discussed in Chapter 2. As the velocity decreases over time, the ability to offer large control forces also decreases. Therefore it is prudent to have most of the corrections done early, when the velocity is still high.

Therefore a $K_p = -4$ is chosen and the transfer function of the full controller is given in Equation 4-6.

$$K(s) = \begin{bmatrix} -4 - 0.4s & 0 \\ 0 & -4 - 0.4s \end{bmatrix} \tag{4-6}$$

Increasing the value of K_p much further is not very helpful. As discussed in Section 3-2-2, the maximum feasible magnitude of the virtual inputs is limited. The maximum actuator force from Table 2-1 is 7.2N at Mach 3. In optimal conditions with an actuator fast enough this results in a maximum virtual input magnitude of

$$\frac{2}{2\pi}7.2 = 2.3N$$

And after just 0.5 seconds this is already reduced to about 1.3N. For slower actuators the maximum possible force is even worse at maximum speed due to the requirement of more complete roll cycles for the input mapping:

$$\frac{2}{6\pi}7.2 = 0.76N$$

As the tracking errors are generally in the order of 0.01-0.4 meters, the required forces would become higher than the maximum possible magnitude and therefore the increase of the controller gains would no longer influence the settling time.

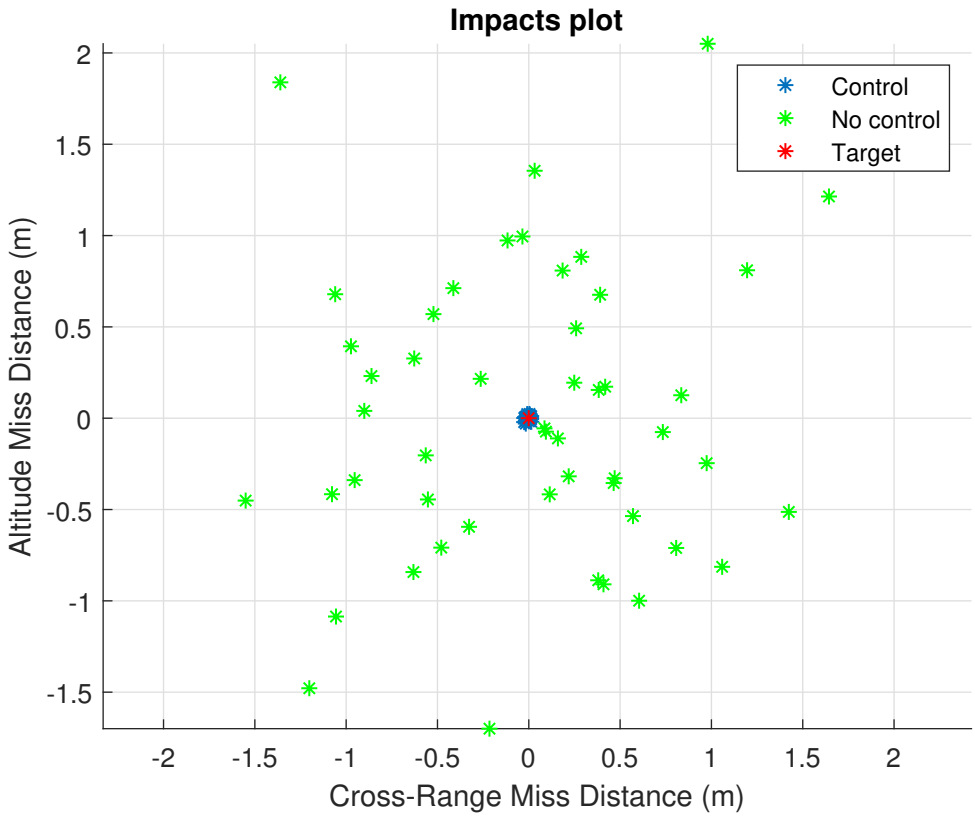

Figure 4-10: Simulated controlled firings using PD-controller

Figure 4-10 shows the impacts of the 50 simulated firings both controlled and uncontrolled. The massive reduction in dispersion is clearly visible. The standard deviation of the projectile impacts is reduced from 0.513 m to 0.007 m and the mean error is reduced from 0.008m to 0.002m.

Chapter 5

Integrated System Results

This chapter will focus on the discussion of the results following the implementation of the entire guidance, navigation and control (GNC) system. The difference between a perfect controller with actual inputs versus the controller with the input transformation is tested. Furthermore an analysis is made to show the influence of the actuator frequency and the projectile spin rate on the performance of the system in order to find the conditions in which the proposed system is able to function at it's best.

5-1 Influence of input transformation

The first thing to be analyzed is the performance of the combined system utilizing the input transformation from Chapter 3 and the controller from Chapter 4. The results in Chapter 4 showed a clear reduction of the standard deviation of the projectile impacts from 0.513 m to 0.007 m and a reduction in the mean error from 0.008 m to 0.002 m. Figure 5-1 shows the impacts for the same 50 firings, but now implemented in a system using the full GNC loop from Figure 3-9.

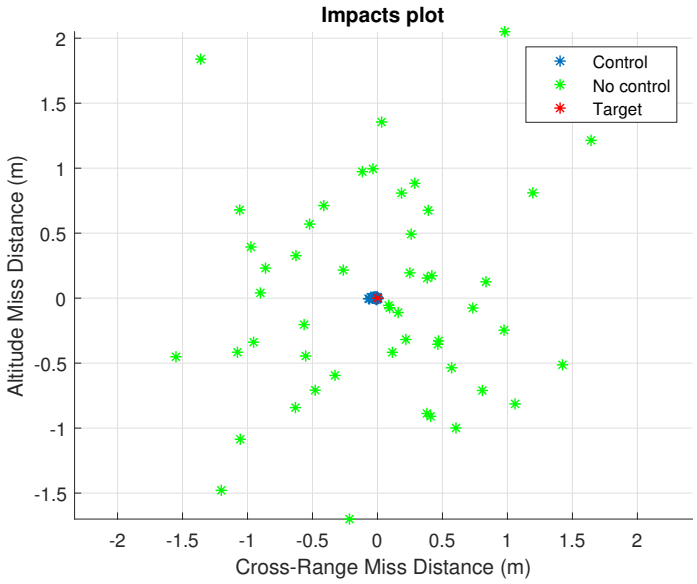

Figure 5-1: Simulated controlled firings $p_0 = 6000$ rad/s, $f = 1000$ Hz

Figure 5-2 shows the same simulation result as Figure 5-1, but now with the results represented by the means and standard deviations.

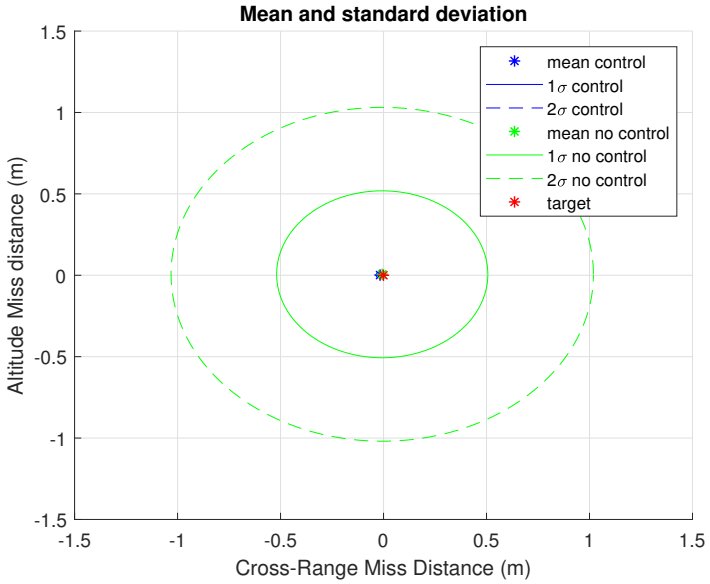

Figure 5-2: Simulated controlled firings standard deviations, $p_0 = 6000$ rad/s, $f = 400$ Hz

As can be seen in the figure, the reduction in standard deviation is still significant with a reduction from 0.513 m to 0.010 m. However, there is now a small increase in the mean error from 0.008 m to 0.017 m. This small increase is negligible when considering the projectile diameter of 0.030 m, especially when also considering the huge gains in the important area of dispersion reduction.

In general, the input transformation is working correctly for the current controller and offers similar results as directly applying the virtual control inputs on the projectile would.

5-2 Influence of actuator frequency and spin rate

The result in Figure 5-1 is based on an input transformation where the actuator is fast enough to fit an entire actuation period in a single roll cycle. In this case for an initial spin rate of $p_0 = 6000$ rad/s and an actuator frequency of 1000 Hz. However, the current actuator is only possible of achieving a frequency of 400 Hz.

For an actuator frequency of 400 Hz and an initial spin rate of 6000 rad/s, the minimum amount of roll cycles to fit the minimum actuation period is 3, following the calculation in Equation 3-7. Because the increase in the required roll cycles decreases the maximum magnitude of the directional force possible, according to Equation 3-8, and increases the instability due to the relatively long periods of open actuator, it is necessary to evaluate the performance for lower frequencies. Therefore, simulations are done using an initial roll rate of 6000 rad/s and an actuator frequency of 400 Hz. Figure 5-3 shows the results with the frequency reduced to this amount and Figure 5-4 is again showing the same simulation result represented by the means and standard deviations.

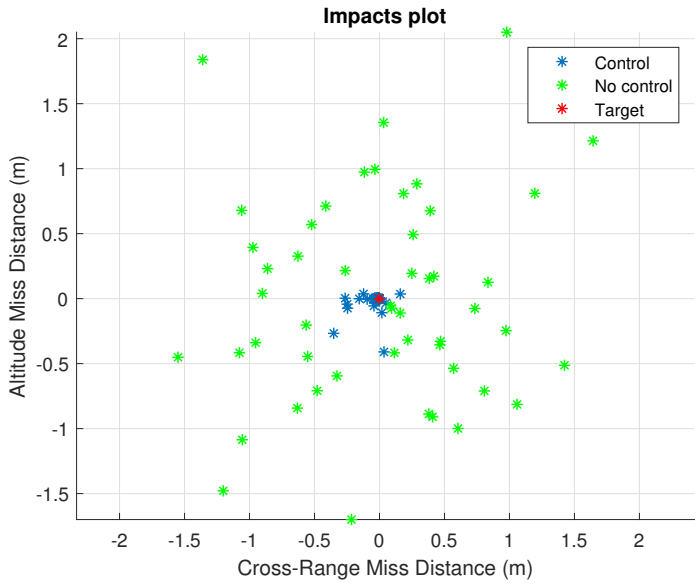

Figure 5-3: Simulated controlled firings $p_0 = 6000$ rad/s, $f = 400$ Hz

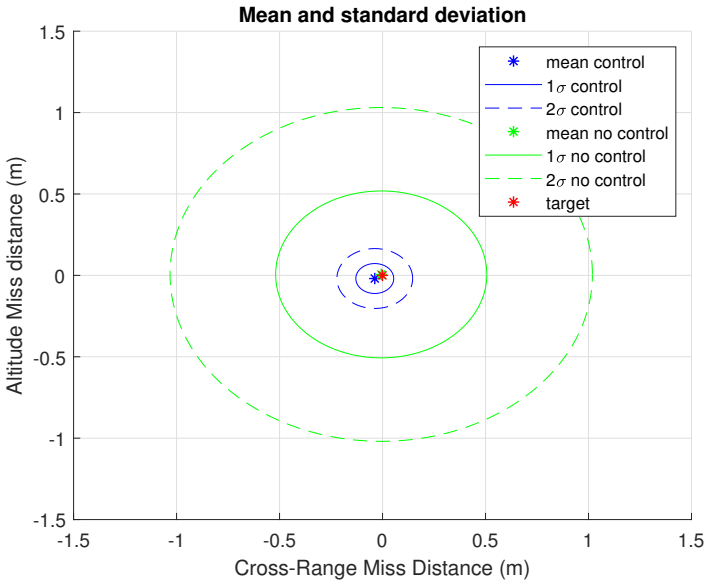

Figure 5-4: Simulated controlled firings standard deviations, $p_0 = 6000$ rad/s, $f = 400$ Hz

With this actuator frequency and spin rate, the mean error of the impacts $\mu_{e_i} = 0.042$ is increased when compared to the uncontrolled firings with $\mu_{e_i} = 0.008$ and the mean error $\mu_{e_i} = 0.016$ of the firings with actuator frequency $f = 6000$ Hz.

The standard deviation of the impacts $\sigma_i = 0.092$ is significantly decreased when compared to the uncontrolled firings with $\sigma_i = 0.513$ but slightly increased when compared to $\sigma_i = 0.010$ for the firings with actuator frequency $f = 6000$ Hz.

5-2-1 Spin rate

Instead of opting to develop faster actuators to match the high spin rates, another strategy is the lowering of the initial spin of the projectile to better match the achievable actuator frequency. Although the stability of the projectile will decrease with lower spin rates, the projectile can be steered easier. Furthermore, the minimum number of required roll cycles N_{min} for the optimization decreases and thus the maximum directional force magnitude increases.

Figure A-1 until Figure A-12 in Appendix A show the impacts represented by their mean and standard deviations for simulations using various combinations of initial spin rate and actuator frequency. The values of these results are also given in Table 5-1.

f(Hz) / p_0(rad/s)	400	600	800	1000
4000	$N_{min} = 2$ $\mu_{e_i} = 0.166$ $\sigma_i = 0.149$	$N_{min} = 2$ $\mu_{e_i} = 0.170$ $\sigma_i = 0.152$	$N_{min} = 1$ $\mu_{e_i} = 0.113$ $\sigma_i = 0.080$	$N_{min} = 1$ $\mu_{e_i} = 0.110$ $\sigma_i = 0.098$
5000	$N_{min} = 2$ $\mu_{e_i} = 0.040$ $\sigma_i = 0.085$	$N_{min} = 2$ $\mu_{e_i} = 0.048$ $\sigma_i = 0.055$	$N_{min} = 1$ $\mu_{e_i} = 0.055$ $\sigma_i = 0.094$	$N_{min} = 1$ $\mu_{e_i} = 0.049$ $\sigma_i = 0.044$
6000	$N_{min} = 3$ $\mu_{e_i} = 0.042$ $\sigma_i = 0.092$	$N_{min} = 2$ $\mu_{e_i} = 0.007$ $\sigma_i = 0.028$	$N_{min} = 2$ $\mu_{e_i} = 0.012$ $\sigma_i = 0.033$	$N_{min} = 1$ $\mu_{e_i} = 0.016$ $\sigma_i = 0.010$

Table 5-1: Performance overview for different spin rates and actuator frequencies (uncontrolled firings achieve $\mu_{e_i} = 0.008$ and $\sigma_i = 0.513$)

From the results of Table 5-1, a few observations can be made:

- Decreasing the actuator frequency f results in a larger standard deviation.
- Variations in the actuator frequency do not influence the mean error significantly.
- The mean error increases significantly with the lowering of the initial spin rate p_0.
- The lowering of the spin rate also increases the standard deviation of the impacts.

All of the results for the fast 6000 rad/s spinning projectile simulations perform better than all of the results for slower spinning projectile simulations. With this in mind, the advice for upcoming innovation would be to focus on increasing the actuator frequency rather than working with the current actuator at lower spin rates. An increase of the current achievable frequency of 400 Hz to a frequency of 600 Hz would yield the most immediate performance improvement.

A small caveat must be made with these results. Most of the control design and tuning is done with the normal 6000 rad/s spin rate in mind. Re-tuning the controller gains with simulations for lower spin rates could improve the results, although the expectation is that these results would still under-perform when compared to the more stable projectiles.

Chapter 6

Conclusion

This thesis research was carried out with the following goal in mind:

Given a medium-sized caliber spinning gun-launched projectile with an actuator developed by TNO, design a guidance and control system that is able to minimize the deviation from the desired impact point for a firing range of 1 kilometer.

After the description of the dynamic models, the structuring of the guidance, navigation and control (GNC) loop with the development of an input transformation and the tuning of a PD-controller, an overall successful guidance and control system that achieves this goal was delivered.

In this final chapter, the main contributions of this research are highlighted followed by a discussion of the limitations of the research accompanied by a few recommendations for further research.

6-1 Contributions

The research done for the sake of this MSc thesis has made a few key contributions:

The development of a simplified model for the actuator prototype in use.

This model describes the magnitude and direction of the actuator force as a function of the projectile velocity V, roll orientation ϕ and the binary input signal u. In combination with a model for the projectile dynamics based on existing research this model forms the framework for all the subsequent development and testing as described in Chapter 2.

The development of an input transformation from one binary input signal to two virtual input forces.

The most important contribution of this thesis is the method for transforming the input signal u to two virtual input forces F_{ay} and F_{az} shown in Chapter 3. This transformation is useful for any actuator that is used to control a spinning projectile by means of transitioning between an on-state and an off-state.

The transformation, based on a discretization of the rolling motion and the solving of an optimization problem, calculates the input signal u that has an equal effect on the projectile as directly applying the forces would have. With this transformation, a few key problems inherent in this setup of actuator and spinning projectile are solved.

The most important benefit is the ability to influence two directions with forces that can be varied in magnitude. In combination with the choice for a guidance method based on the pre-launch calculation of the preferred trajectory, this method allows for the use of simpler controllers that don't require complete information or linearization of the highly nonlinear projectile model.

PD-controller design

Chapter 4 focused on the development of a controller that serves to track the predefined trajectory. Using the newly created virtual inputs, two separate control loops with equal PD-controllers can be used to achieve this tracking. The optimal controller that minimize the sum of the average error and the standard deviation is found with a grid-search.

Thereafter, the influence of the spin rate and the actuator frequency on the overall system performance is evaluated in Chapter 5. Performance for the system is at it's best when a combination of high spin rates and high actuation frequency is used. A recommendation for a focus on the increase of the actuator frequency is therefore issued when the current prototype will be used with the proposed system.

6-1-1 Scope

The results of this thesis offer a starting point for the implementation of the novel actuation system for the use in spinning projectiles. It offers a basic system framework that proves that the actuator that is currently being developed for non-spinning systems also has a benefit when used in a spinning system. At the very least, the system is capable of removing the dispersion resulting from internal variations.

On a larger scale, with these novel fin-less actuation systems becoming more viable for the control of smaller projectiles, the deployment of controlled projectiles could become more likely. The high costs and need for specially developed launch mechanisms for fin-controlled projectiles have been large obstacles and thus the switch to a likely cheaper alternative that doesn't require new launch mechanisms could accelerate the process.

6-2 Discussion

A few remarks need to be made on the applicability of the results of this research. Although a guidance and control strategy was successfully developed, the system is still limited in it's use.

6-2-1 Limitations

There are a few main limitations that should be highlighted when considering the implementation of the results:

- As discussed in Chapter 3, the navigation part of the GNC loop is considered to be delivering completely accurate information on the projectile states. In reality, the measurement and estimation of these states will require more thought. Sensor noise, time delays and problems with the integration of the navigation in the system will become significant for real-time use. An especially important issue will be the estimation of the current roll angle ϕ, as it directly influences the validity of the input transformation.
- The input of the controller was simplified by the omission of the actual electric circuit with inductor that is used to drive the actuator state u. The choice for the actuator state as the manipulable variable means that the time delays and other dynamics are not considered. This is not necessarily an issue for simulations, but problems could arise in real-world application.
- The controller design lacks the analytical depth to prove overall optimality. For the given system, initial conditions and guidance strategy, the chosen controller gains for a PD-controller are close to the optimal gains in the set of gains that is considered. However, due to the inability to acquire useful linearizations and the complicated projectile model, other possible control techniques that could potentially provide better results are not evaluated.

  Furthermore, the controller is tuned for the specific firing range of 1 km. Shorter distances may require higher gains. Higher distances, although not common for these projectiles, would require the use of multiple controllers or adaptive controllers due to the transition from supersonic to subsonic velocities.

6-2-2 Recommendations for further research

When considering all of the contributions and limitation of this thesis, there are some areas that would benefit most from further research.

- The optimization done during the input transformation in Chapter 3 is relatively inefficient. Due to the complicated constraints that are put on the input signal that is to be mapped, resultant forces corresponding to all of the possible input signals have to be calculated before finding the optimal one. Further research on rewriting these constraints in a more efficient way to make optimization techniques such as nonlinear integer programming possible would considerably speed up the process and make the system more suitable for real-time implementation.

- Further research that evaluates the performance of other controllers for the system following the input transformation. A working linearized model was not obtained. Obtaining such a model could allow for more model-based or optimal control strategies. Additionally, nonlinear control strategies could also be evaluated to further seek the best performing solution.
- Most importantly, research must be done on the disturbance rejection capabilities of the system. Currently, the system is able to compensate for the dispersion resulting from internal variations. This alone offers huge benefits, but when external disturbances such as wind and sensor noise can also be compensated for, the usefulness of the system will increase significantly.

Appendix A

Figures

A-1 Standard deviations for different actuator frequencies and spin rates

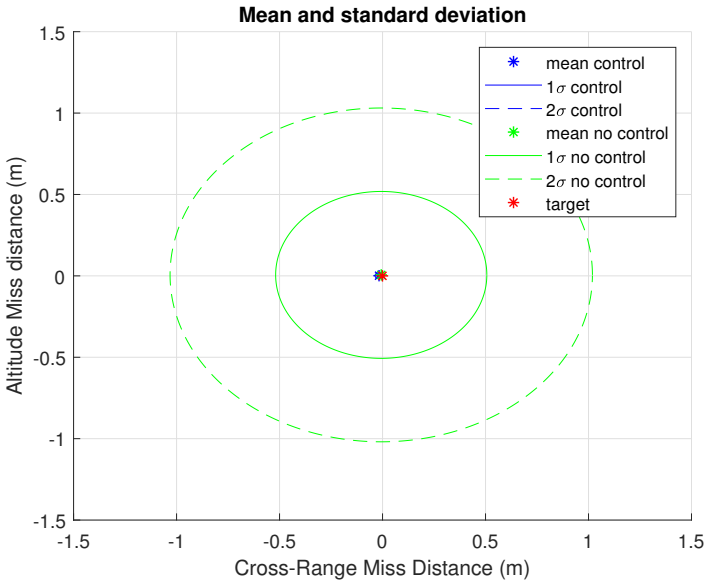

Figure A-1: Simulated controlled firings standard deviations, $p_0 = 6000$ rad/s, $f = 1000$ Hz

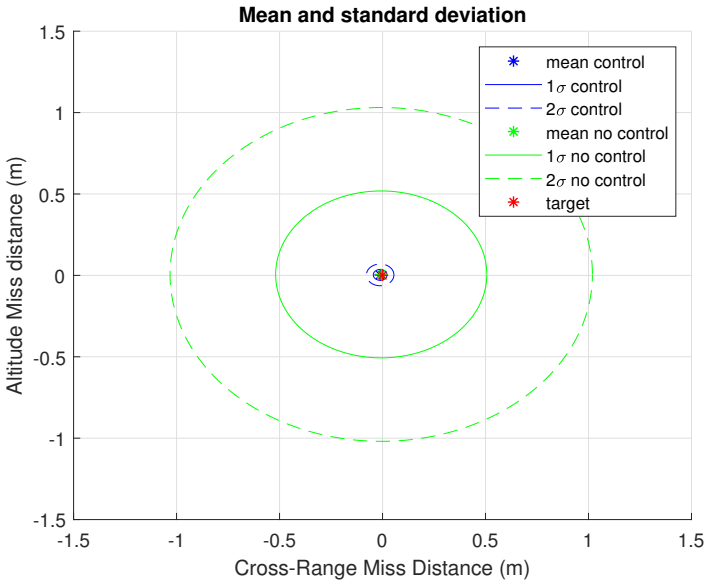

Figure A-2: Simulated controlled firings standard deviations, $p_0 = 6000$ rad/s, $f = 800$ Hz

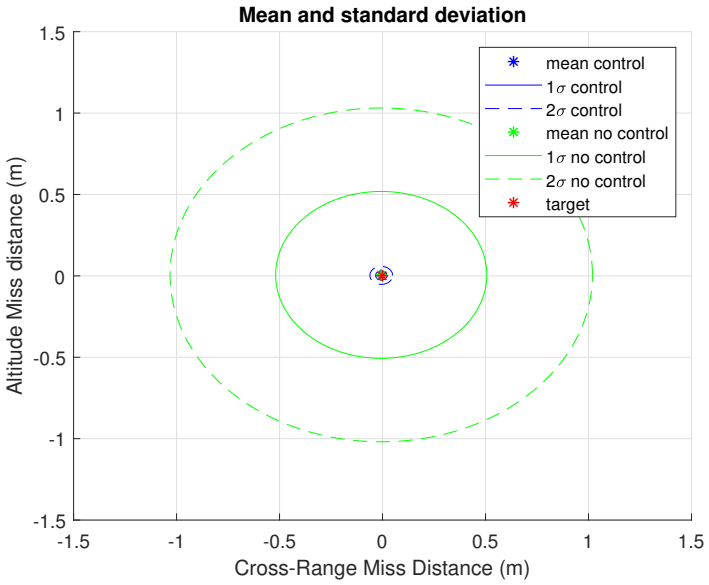

Figure A-3: Simulated controlled firings standard deviations, $p_0 = 6000$ rad/s, $f = 600$ Hz

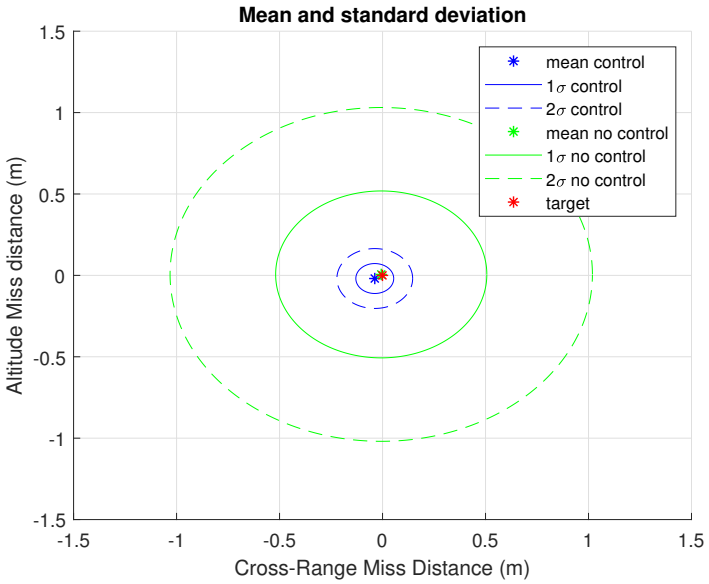

Figure A-4: Simulated controlled firings standard deviations, $p_0 = 6000$ rad/s, $f = 400$ Hz

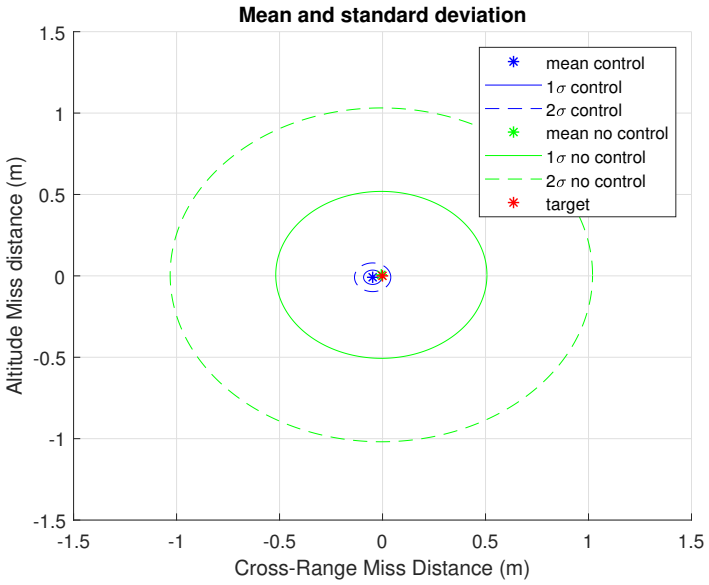

Figure A-5: Simulated controlled firings standard deviations, $p_0 = 5000$ rad/s, $f = 1000$ Hz

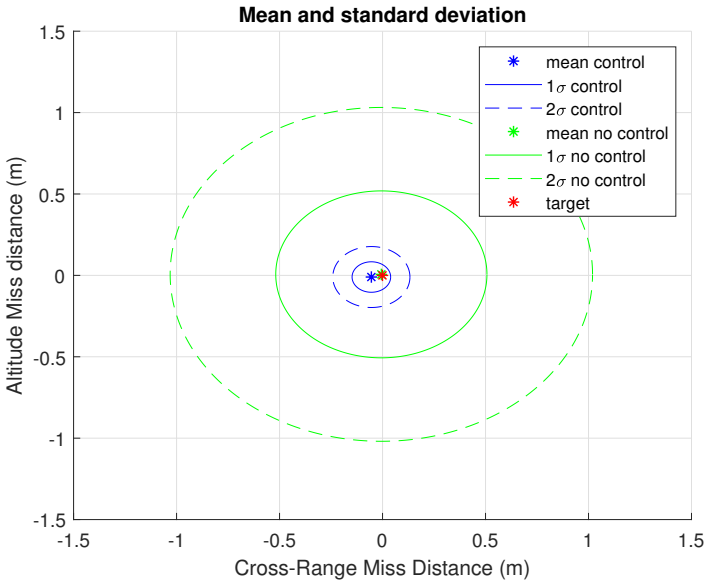

Figure A-6: Simulated controlled firings standard deviations, $p_0 = 5000$ rad/s, $f = 800$ Hz

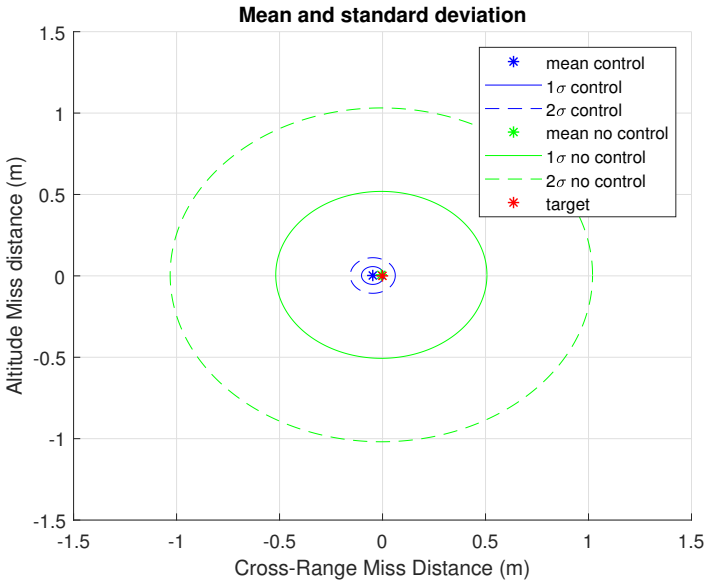

Figure A-7: Simulated controlled firings standard deviations, $p_0 = 5000$ rad/s, $f = 600$ Hz

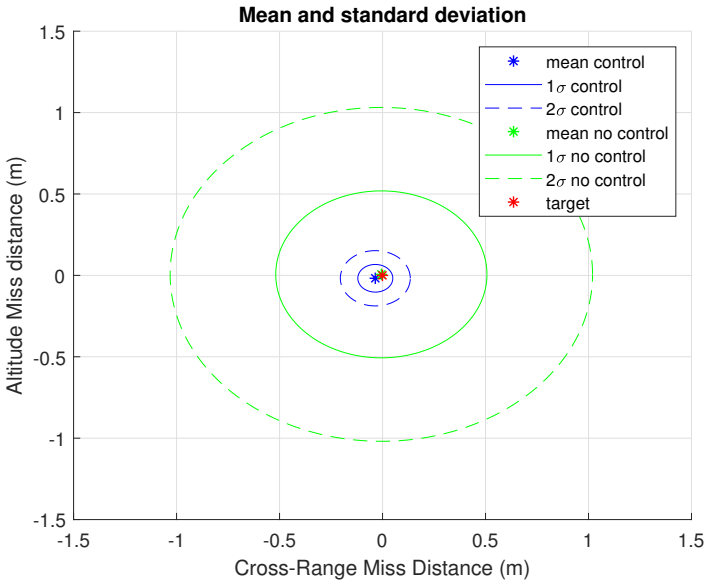

Figure A-8: Simulated controlled firings standard deviations, $p_0 = 5000$ rad/s, $f = 400$ Hz

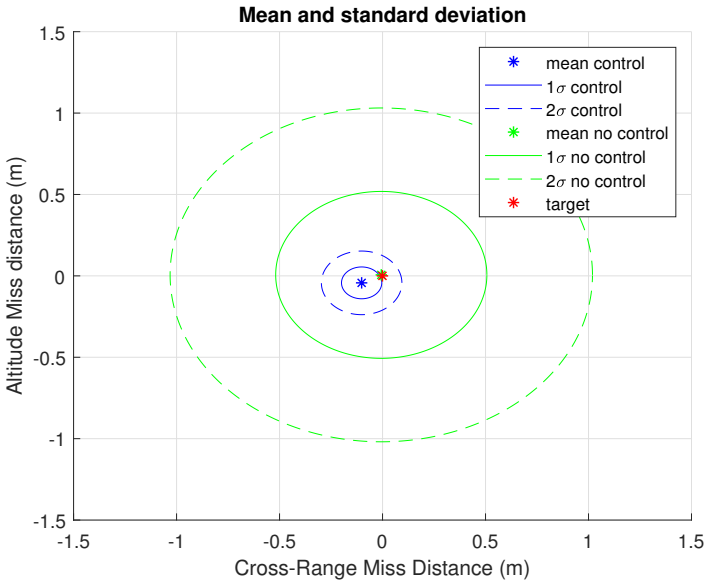

Figure A-9: Simulated controlled firings standard deviations, $p_0 = 4000$ rad/s, $f = 1000$ Hz

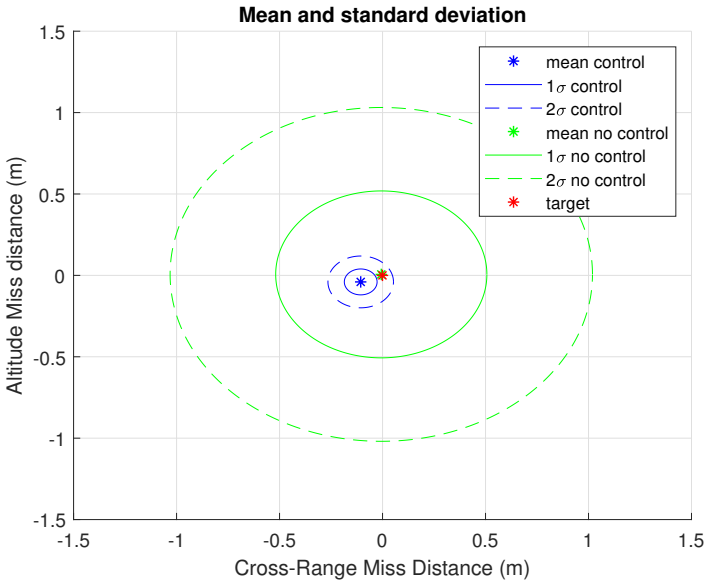

Figure A-10: Simulated controlled firings standard deviations, $p_0 = 4000$ rad/s, $f = 800$ Hz

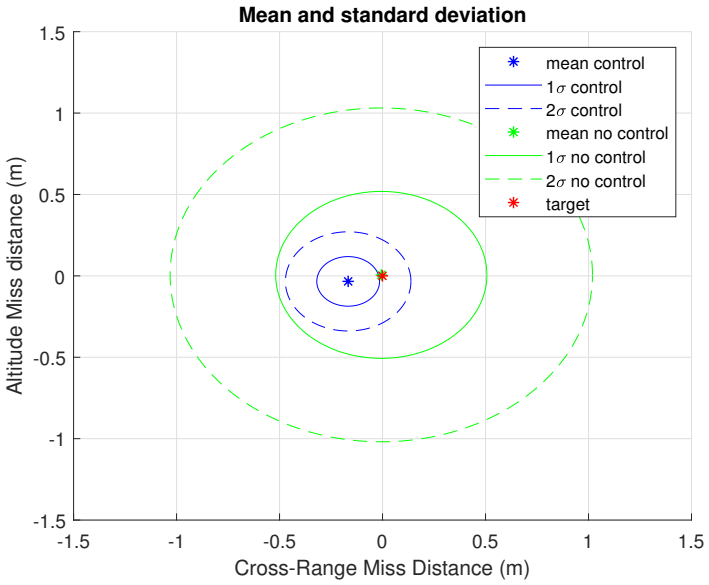

Figure A-11: Simulated controlled firings standard deviations, $p_0 = 4000$ rad/s, $f = 600$ Hz

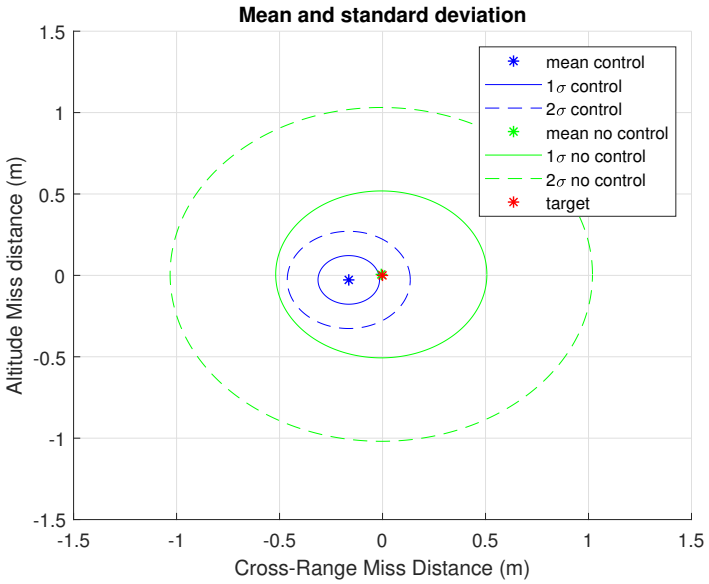

Figure A-12: Simulated controlled firings standard deviations, $p_0 = 4000$ rad/s, $f = 400$ Hz

Appendix B

Tables

B-1 Aerodynamic Coefficients

Mach	C_X0	C_X2	C_Na	C_Ypa	C_lp	C_Mq	C_Ma	C_npa
0.01	0.1819	2.04	2.023	-0.59	-0.02808	2.5	2.576	-1.636
0.4	0.1784	2.04	2.07	-0.59	-0.0268	2.6	2.56	-1.636
0.6	0.1831	2.04	2.067	-0.59	-0.02637	2.3	2.555	-1.636
0.7	0.1871	2.26	2.06	-0.59	-0.02622	2	2.553	-1.718
0.75	0.19	2.36	2.068	-0.6	-0.02612	1.8	2.563	-1.632
0.8	0.2009	2.46	2.098	-0.61	-0.02576	1.6	2.644	-1.454
0.85	0.2144	2.53	2.119	-0.63	-0.0256	1.5	2.629	-1.215
0.875	0.2359	2.6	2.179	-0.64	-0.02545	0.9	2.666	-1.058
0.9	0.2664	2.68	2.265	-0.66	-0.02526	-0.2	2.729	-1.044
0.925	0.3088	2.79	2.336	-0.74	-0.02494	-1.7	2.813	-0.987
0.95	0.355	2.9	2.426	-0.85	-0.02467	-3.2	2.933	-0.864
0.975	0.4202	3.05	2.575	-0.75	-0.02465	-4.5	2.976	-0.624
1	0.4959	3.23	2.651	-0.69	-0.02465	-5.5	2.924	-0.509
1.025	0.5322	3.41	2.591	-0.66	-0.02421	-6.4	2.86	-0.365
1.05	0.5585	3.66	2.596	-0.63	-0.02356	-6.8	2.78	-0.301
1.1	0.5602	4.07	2.575	-0.59	-0.02155	-7.2	2.631	-0.151
1.2	0.5614	4.5	2.627	-0.53	-0.01905	-8	2.482	-0.07
1.35	0.5436	3.94	2.615	-0.48	-0.01813	-8.2	2.328	0.012
1.5	0.527	3.43	2.649	-0.46	-0.01856	-7.6	2.08	0.124
1.75	0.4969	2.9	2.746	-0.44	-0.01806	-6.8	1.77	0.123
2	0.4664	2.34	2.889	-0.41	-0.01694	-6.3	1.524	0.131
2.25	0.4398	2.11	2.958	-0.41	-0.01614	-5.8	1.335	0.125
2.5	0.417	1.89	2.976	-0.41	-0.01543	-5.7	1.253	0.122
3	0.382	1.47	2.977	-0.41	-0.01434	-5	1.177	0.118
3.5	0.3611	1.29	2.941	-0.41	-0.01367	-4	1.264	0.118
4	0.3509	1.14	2.855	-0.41	-0.01354	-3.2	1.363	0.118
4.5	0.3385	0.99	2.798	-0.41	-0.0133	-2.7	1.402	0.118
5	0.3279	0.84	2.748	-0.41	-0.01312	-2.2	1.428	0.118
6	0.3115	0.74	2.674	-0.41	-0.01289	-1.6	1.441	0.118
8	0.2985	0.69	2.623	-0.41	-0.01299	-1.5	1.316	0.118

Table B-1: Table containing the Aerodynamic Coefficients found using PRODAS

Bibliography

[1] R. L. McCoy, *Modern Exterior Ballistics: The Launch and Flight Dynamics of Symmetric Projectiles (Revised 2nd Edition)*. Schiffer Publishing, 2012.

[2] L. C. Hainz and M. F. Costello, "Modified projectile linear theory for rapid trajectory prediction," *Journal of Guidance, Control and Dynamics*, vol. 28, no. 5, pp. 1006–1014, 2005.

[3] J. Rogers and M. F. Costello, "A low-cost orientation estimator for smart projectiles using magnetometers and thermopiles," *Journal of The Institute of Navigation*, vol. 59, no. 1, pp. 9–24, 2012.

[4] D. N. Gkritzapis, E. E. Panagiotopoulos, D. P. Margaris, and D. G. Papanikas, "Modified linear theory for spinning or non-spinning projectiles," *The Open Mechanics Journal*, vol. 2, pp. 6–11, 2008.

[5] J. D. j. Anderson, *Fundamentals of Aerodynamics: Fifth Edition in SI Units*. McGraw-Hill, 2011.

[6] "Normal shock wave." https://www.grc.nasa.gov/www/k-12/airplane/normal.html. Accessed: 01-02-2019.

[7] J. Zhu, P. Wu, and Y. Bo, "A novel attitude estimation algorithm based on the non-orthogonal magnetic sensors," *Sensors*, vol. 16, no. 5, 2016.

[8] J. Rogers and M. F. Costello, "Effective use of magnetometer feedback for smart projectile applications," *Journal of The Institute of Navigation*, vol. 58, no. 3, pp. 203–219, 2011.

[9] J. Rogers and M. F. Costello, "Roll orientation estimator for smart projectiles using thermopile sensors," *Journal of Guidance, Control and Dynamics*, vol. 34, no. 3, pp. 688–697, 2011.

[10] T. E. Harkins, "Understanding body-fixed sensor output from projectile flight experiments," tech. rep., U.S. Army Research Laboratory, 2003.

[11] D. J. Hepner and T. E. Harkins, "Determining inertial orientation of a spinning body with body-fixed sensors," tech. rep., U.S. Army Research Laboratory, 2001.

[12] S. Changey, V. Fleck, and D. Beauvois, "Projectile attitude and position determination using magnetometer sensor only," in *Proceedings of the SPIE*, vol. 5803, pp. 49–58, 2005.

[13] B. Allik, M. Ilg, and R. Zurakowski, "Ballistic roll estimation using ekf frequency tracking and adaptive noise cancellation," *IEEE Transactions of Aerospace and Electronic Systems*, vol. 49, no. 4, pp. 2546–2553, 2013.

[14] J. M. Maley, "Efficient attitude estimation for a spin-stabilized projectile," *Journal of Guidance, Control and Dynamics*, vol. 39, no. 2, pp. 339–350, 2016.

[15] F. Fresconi, I. Celmins, and S. I. Silton, "Theory, guidance, and flight control for high maneaverability projectiles," tech. rep., U.S. Army Research Laboratory, 2014.

[16] D. Ollerenshaw and M. Costello, "On the swerve response of projectiles to control input," *Journal of Guidance, Control and Dynamics*, vol. 31, no. 5, pp. 1323–1333, 2008.

Glossary

List of Acronyms

3-DOF	three degrees of freedom
4-DOF	four degrees of freedom
6-DOF	six degrees of freedom
AOA	angle of attack
CFD	computational fluid dynamics
COM	center of mass
COP	center of pressure
EKF	Extended Kalman Filter
GNC	guidance, navigation and control
IPC	Innovative Projectile Control
IPP	impact point prediction
MPC	model predictive control
PNG	proportional navigation guidance
YPR	yaw-pitch-roll